NTNU – Trondheim
Norwegian University of
Science and Technology

The Influence of Ni and V Trace Elements on the High Temperature Tensile Properties of A356 Aluminium Foundry Alloy

Maria Teresa Di Giovanni

Materials Technology
Submission date: June 2014
Supervisor: Lars Arnberg, IMTE

Norwegian University of Science and Technology
Department of Materials Science and Engineering

Abstract

In this work, the High temperature tensile properties of unmodified A356 alloys with trace additions of Ni or V were investigated by analysing samples obtained from sand and permanent casting in as-cast and T6 heat treated conditions. Trace elements were added in concentrations of 600 and 1000 ppm of Ni and V, respectively. High temperature tensile tests were performed at 235°C and crosshead speed was 1mm/min. A comparison between the High and the Room temperature mechanical properties was also carried out. It was found that neither Ni nor V addition exercises a detrimental effect on the High temperature tensile properties. Unlike what was expected, the references and Ni-containing sand and permanent mould cast alloys, in the as-cast condition, shown an increase in yield strength at High temperature as compared to the Room temperature. The phenomenon of V solid solution strengthening stated at Room temperature, was discovered to be less efficient at High temperature. The strength of the alloys in the T6 condition, in both sand and permanent mould castings shown a small decrease at High temperature as compared to the Room temperature, it was most likely due to the over-aging. Under the High temperature condition the α-Al matrix was more capable to be deform, the internal stress originated by the non- homogeneity, induced by the presence of the acicular eutectic Si crystals, was partially recovered at the expense of the matrix. Hence fracture occurred at lower strength values compared with the room temperature case, but offered higher elongation.

Contents

1 Introduction

The use of light-metal alloys in various applications such as automotive and aerospace has recently increased because of their good castability, lightness, low strength-to-weight ratio and corrosion resistance. Al-Si-Mg foundry alloys are found to give good results since they show excellent casting characteristics and mechanical properties. Higher strenth can be eventually achieved by heat treatment involving solutioninsig and subsequent age hardening. Though, a growing concern is the deterioration in the current coke quality for anode production, which is necessary for the Hall-Héroult electrolytic process. This has led to increase the amount of metal impurities such as Ni and V in primary aluminium. In the next years, the levels of Ni and V are expected to rise to 420 and 1080 ppm, respectively. At the present, there is no cost effective or efficient method available for removal of these impurities, and the response to the problem is mainly monitoring the V and Ni levels and checking for any negative influence [1]. Therefore industries are developing a growing interest with respect to the effect of increased Ni and V levels on the downstream properties of aluminium alloy products.

A previous study [2] investigated the room temperature tensile properties of sand cast and permanent mould cast unmodified A356 alloy containing 600 and 1000 ppm of Ni and V, respectively. It was found that Ni and V strongly affect both the yield strength (Rp_{02}) and ultimate tensile strength (UTS) of the sand cast alloy in the as-cast condition, in particular, Ni reduce Rp_{02} and UTS by 87% and 37% respectively whereas V addition increases Rp_{02} and UTS by 42% and 25%.

In the last decade, aluminium alloys has been re-focused in term of lightweight material for vehicles. Replacing cast iron with aluminium alloys can result in a significant weight reduction and consequently better fuel efficiency [3]. Considering the new trends it might be interesting to understand which role is played by the Ni- and V- addition on the High temperature mechanical behaviour. High-Temperature performance is a critical characteristic affecting an alloy's suitability for various automotive power-train applications. Diesel cylinder heads for passenger cars and light trucks are particular challenging examples. Contemporary automotive engines operate at higher temperatures reaching up to 250° C and peak pressure up to 180 bar for improved gasoline consumption and reduced Green House Gas (GHG) emissions [4]. This creates demanding operating requirements for existing Al-Si-Cu and Al-Si-Mg alloy that typically lose strength above 150°C. Much development and many studies are still ongoing for the purpose of improving heat-resistant stability, high temperature mechanical and fatigue properties. Recent studies investigated complex hypoeutectic and near eutectic Al-Si based alloys, with the aim to improve their properties

for high temperature applications [5-9]. Heusler *et al.* [5] proposed a new alloy for engine applications based on the Al-Si-Mg-Cu-Fe-Ni system, they showed an increase in fatigue properties and tensile strength at High temperature attributed to the present of Fe-bearing intermetallic compounds. Ashgar *et al.* [6] reported a significant elevated-temperature strength in Al-12SiNi, where the addition of 1.2 wt% Ni led to the formation of an interconnected hybrid reinforcement consisting of eutectic Si and Ni and Fe aluminides. Conversely there is a lack of information about the effect of V addition with respect to High temperature tensile properties of the Al-Si-Mg alloy system. It was recently observed that V is added in combination with Zr (or Ti) in order to stabilise the mechanical properties in both room and high temperatures through the formation of Al_3X trialuminide phases during the ageing stage of the heat treatment [10-12]. Further details are given in [2].

Currently, only the EN 1676-2010 standard specifies the maximum concentration limit for V of 0.03wt% for EN-AB aluminium foundry alloys, which correspond to A356 commercial alloys. On the other side there are no indications for the maximum tolerable Ni level in this group of alloys. Hence the objective of this work is to evaluate the influence of Ni and V trace elements on the High temperature tensile properties of as-cast and T6 heat treated A356 unmodified foundry alloys in both sand and permanent mould casting process. This study also proposes an indication about the tolerable levels of Ni and V for the High temperature applications of the much-used A356 aluminium foundry alloys, in the case in which the Ni- or V- containing alloys show mechanical properties comparable to the base alloy. High Temperature tensile tests were performed to evaluate the mechanical properties. Further, microstructural and fractographic investigations were carried out to analyse the microstructures features involved in the fracture process.

2 Theoretical Background

2.1 Al-Si foundry alloys

2.1.1 Introduction

Al-Si foundry alloys are widely used in the automotive and aerospace industry due to their good castability, lightness, low strength-to-weight ratio and corrosion resistance.
Silicon increases the fluidity in aluminium casting alloys, reduces the melting temperature and the thermal expansion coefficient and diminishes the tendency of the alloy toward shrinkage and hot tearing. The Al-Si system is a simple eutectic system. The two solid solution phases are FCC Al and Diamond-cubic Si (Figure 2.1).
Al-Si alloys are divided into three groups:
1. Hypoeutectic containing 5-10% silicon
2. Eutectic containing 10-13% silicon
3. Hypereutectic containing 13-25% silicon

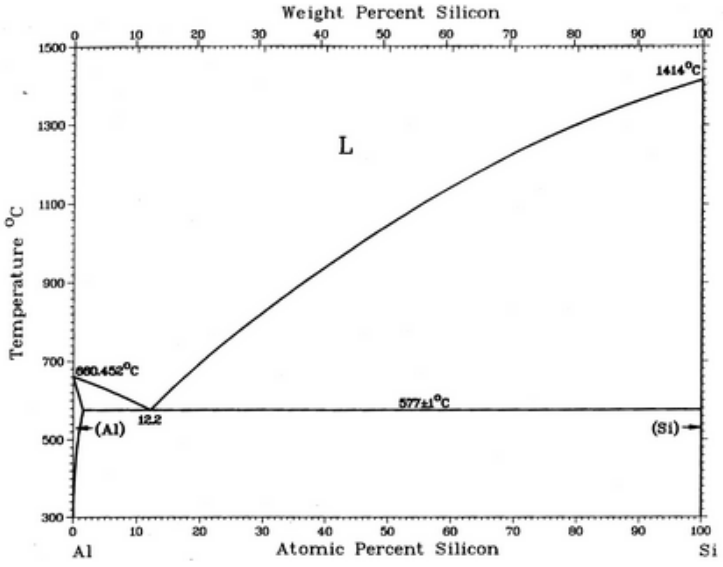

Figure 2.1- *Phase diagram of the binary Al-Si system. [13]*

Depending on the purity of the base material, the Al-Si alloys contain varying amounts of impurity elements like Fe, Mn, Cu and Zn. Cu and Mg are often added as alloying elements to increase the strength and the hardenability of the castings.
Al-Si foundry alloys are generally hypoeutectic.

The maximum solubility of Si in Al is 1.5 at% at the eutectic temperature of 577° C.
The solubility of Al in Si is negligible. [14]
The solidification of hypoeutectic alloys starts with the formation of primary α-Al dendrites, minor dendrite branches on the primary dendrites also grow in the liquid. The dendrites stop growing as soon as the temperature of the melt reaches the eutectic temperature, when an interconnected network is formed. After further cooling, the content of Si in the residual liquid, rejected by the primary phase, will eventually increase and, when the undercooling is sufficiently large the final eutectic reaction occurs.
In the end, the precipitation of secondary eutectic phases such as Mg_2Si and Al_2Cu, can be observed.
In contrast to the previous alloys, the solidification of hypereutectic alloys starts by the nucleation of polyhedral primary Si crystals and ends with the subsequent eutectic reaction.
Commercial Al-Si alloys contain between 5 to 20 wt% Si. These alloys have a eutectic volume fraction ranging between 50-100% and considering that most of the casting defects originate in the later stages of solidification, the eutectic reaction is of great importance as it will strongly influence the alloys' mechanical properties. Alloys in which Si-particles are small, round and uniformly distributed are usually displaying high ductility [15]. In addition to the main reaction, precipitation of iron- and manganese- containing phases will take place, the most common of such phases in foundry alloys are Al_5FeSi and $Al_{15}(Mn, Fe)_3 Si_2$ [16].

2.1.2 The A356 alloy

Alloy A356 is a high-purity version of the well-known casting alloy 356, and belongs to a group of hypoeutectic Al-Si alloys. It is designed as EN AB-42100, according to the EN 1676-2010 specifications. Chemical composition are given in Table 2.1
The as-cast microstructure consists of primary dendrites of α-Al containing magnesium and silicon in solution, surrounded by an Al/Si eutectic phase. The size and morphology of the eutectic silicon depends on the casting conditions, as well as the presence of chemical modifiers such as strontium, sodium or antimony. Without modification the eutectic silicon forms as coarse platelets, shown in Figure 2.2 - a, whereas a fine 'fibrous' or 'coral-like' structure occurs in modified alloys, Figure 2.2 - b. Other phases found in commercial A356 alloys include Mg_2Si particles, which are taken into solid solution and precipitated during heat treatment, and Fe-rich phases including α-Al_5SiFe, β-Al_8Si2Fe and π-Al8Mg3Si6Fe that arise from the presence of melt impurities. The presences of the

Fe-bearing compounds influence the ductility of the alloy [17]. Their volume and shape depend on the Mg content [18-19] and on the cooling rate respectively.

In most cases the alloy is subject to heat treatment, and as a result, several combinations of tensile and other mechanical properties can be provided. Due to low iron and impurity content, high ductility can be achieved. The alloy is generally used for aircraft structures, cast aluminium automobile wheels and structural components [16].

Table 2.1- *Chemical composition of the A356 foundry alloy in accordance with EN 1676-2010 specification. No specific information about the maximal tolerable Cr, Ni, Pb and Sn concentration is given.*

A 356 - EN AB-42100	
Element	**Composition [wt%]**
Si	6.50 -7.50
Mg	0.30 -0.45
Fe	0.15
Cu	0.03
Mn	0.10
Zn	0.07
Ti	0.18
Other	0.03(each) 0.10(total)
Al	bal.

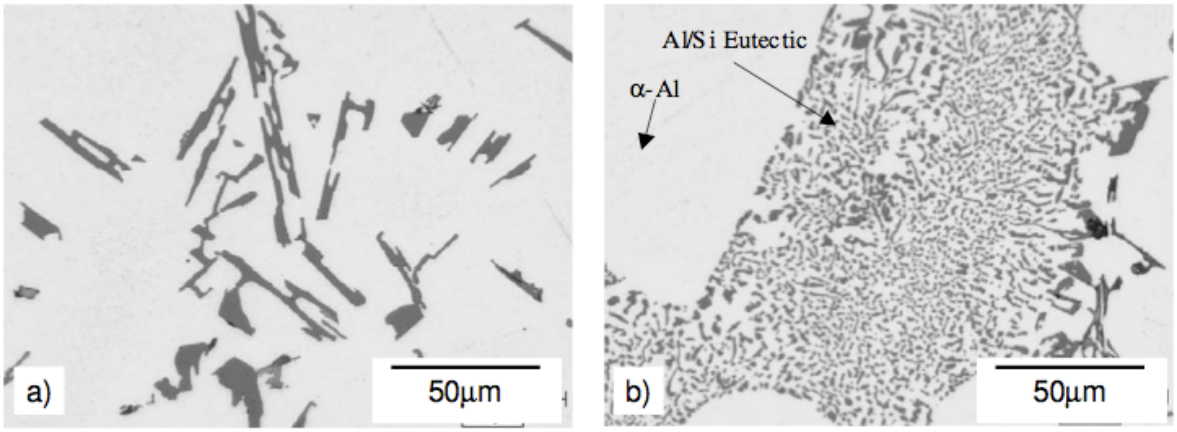

Figure 2.2 - *Microstructure of Al/Si eutectic phase in an as-cast A356 aluminium alloy; (a) Unmodified alloy, (b) Modified with an addition of 156ppm strontium [20].*

2.1.3 Microstructure

The solidification sequence is reported as follows:

- T= 610°C – Start of solidification and formation of α-Al dendrites
- T= 568°C – Start of main eutectic reaction: Liq. $\rightarrow$ Al + Si + Al_5FeSi
- T= 557°C – Precipitation of Mg_2Si: Liq. $\rightarrow$ Al + Si + Mg_2Si
- T= 550°C – Precipitation of complex eutectic: Liq. $\rightarrow$ Al + Si + Mg_2Si + $Al_8Mg_3FeSi_6$

According to Arnberg et al. [16], the nucleation of α-Al starts at 610°C. Equiaxed dendritic crystal begins evolving, and become coherent at 604°C. The eutectic reaction starts at 568°C, and the fist β-Al_5FeSi platelets begin to appear. Under continued solidification the Mg_2Si phase and the π-$Al_8Mg_3FeSi_6$ phase precipitate.

2.2 Heat Treatment

2.2.1 The influence of Mg in A356 alloy

Mg is added into the A356 foundry alloy with the purpose of inducing age hardening through the precipitation of fine Mg_2Si particles [21]. It is believed that while Mg achieves the pursuit of making the aluminium matrix age-hardenable, it might affect the microstructure and in particular the type and morphology of brittle phases and consequently a decrease in ductility and fracture toughness appears [19, 22]. According to Shivkumar *et al.* [23], the sequence of precipitation in the commercial A356 foundry alloy can be described as follows:

- Precipitation of GP zones (needles ~ 10 nm long);
- Intermediate phase β''- Mg_2Si, (homogeneous precipitation);
- Intermetallic phase β'- Mg_2Si, (heterogeneous precipitation);
- Equilibrium phase β- Mg_2Si, FCC structure (a=0.639), rod or plate-shaped.

Supersatured solid solution (SSSS) decomposes as Mg and Si atoms are attracted first by themselves (cluster), then to each other forming precipitates GP, or sometimes β''- Mg_2Si. GP zone consist of alternating arrangement of Mg and Si atoms columns along the $\langle 100 \rangle_\alpha$ direction. GP zones can also evolve directly to phase β'' and then to a number of other metastable phases labelled β', B', U1, U2 (Figure 2.3) .The peak aging (the maximum alloy strength) is enriched just ahead of the incoherent β- platelets precipitation. The precipitation of metastable Mg-rich phases depends on the Mg-to-Si ratio. The excess of Si in solid solution can significantly alter the kinetics

of precipitation and the phase composition. Equilibrium phases are enriched in Mg and metastable phases are enriched in Si [24].

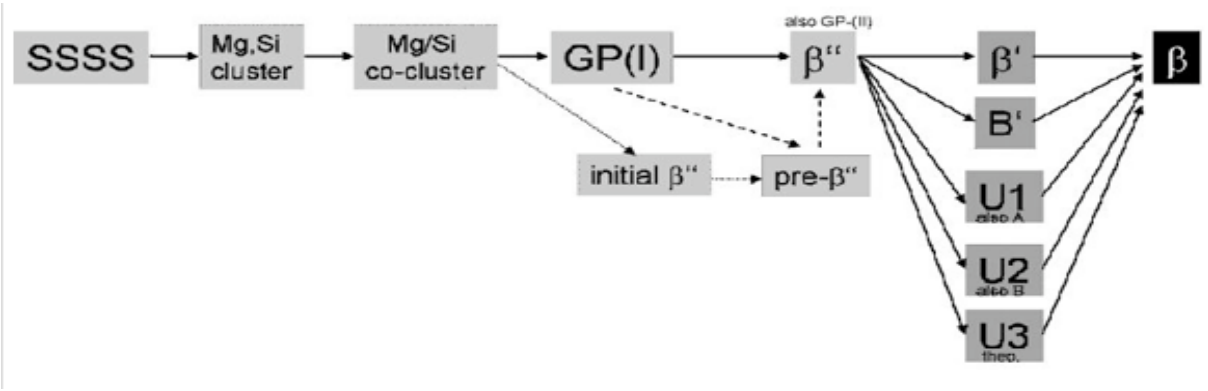

Figure 2.3- *Supersatured solid solution (SSSS) decomposes as Mg and Si atoms are attracted first by themselves (cluster), then to each other developing in precipitates GP, or sometimes β'' - Mg_2Si. GP zones can also evolve directly to phase β'' and then to a number of other metastable phases labelled β', B', U1, U2* [24].

2.2.2 The T6 heat treatment

Controlled heat treatment of aluminium alloys can significantly influence properties such as strength, ductility, toughness, and corrosion resistance, as well as the formation of residual stresses and the thermal and dimensional stability of the component. The main heat treatment process applied to cast Al-Si-Mg alloys is precipitation hardening. The standard procedure for T6 heat-treatment consists of three stages (Figure 2.4):

- Solution treatment at high temperature
- Quenching
- Age Hardening

Solution treatment requires long soak times at high temperature in order to produce a homogeneous solid solution with maximum solute concentration. The soak temperature is determined by alloy composition and solid solubility limit, and is generally close to the eutectic temperature of the alloy (475-566°C) [24].

Underheating can result in incomplete dissolution of particles, low solute concentrations, and inhomogeneous solute distributions in the matrix; all of which cause a reduction in the strengthening potential of the alloy. During this stage, phases that have been formed during the solidification such as Mg_2Si and the Fe- rich phases (slow-diffusing) progressively dissolve. Another significant metallurgical process during solution treatment is the change in shape of insoluble second phase particles. In the case of Al-Si-Mg alloys this involves a change in the

eutectic Si crystals from the as-cast structure to spheroidal globules (Figure 2.5).

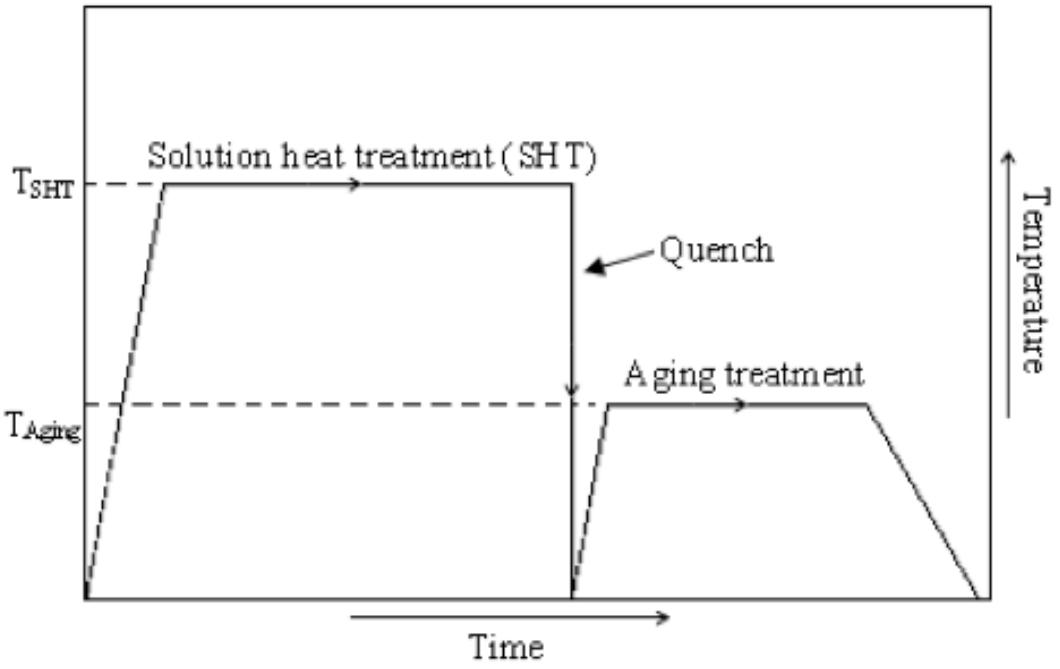

Figure 2.4 – *Diagram showing the three steps for precipitation hardening [24].*

Homogenization of the casting to attain a globular morphology of the eutectic Si is of primary importance to improve ductility and fracture toughness.

After the dissolution process, the alloy must be rapidly cooled to produce a highly supersaturated solid solution containing large numbers of "quenched-in" vacancies [25]. The greatest benefit from the standpoint of alloy properties is achieved with the fastest quench as it ensures the maximum supersaturated solute concentration, but, on the other side, lattice residual stresses can develop, affecting the ductility.

During the age-hardening stage a fine dispersion of second phase particles precipitates from a supersaturated solid solution. This can be realised by exposing the alloy to a suitable combination of temperature and time. Typically, precipitation reactions involve the formation of intermediate phases prior to the equilibrium phase, each of which influences the overall strength. There are two different methods of ageing, natural and artificial aging.

Natural ageing refers to the decomposition of a supersaturated solid solution over time at room temperature following quenching. Depending on the alloy, natural ageing occurs over a few hours to several years, and results in an increase in strength from the as-quenched condition due to the

formation of solute clusters or GP zones.

The decomposition of a supersaturated solid solution at elevated temperature is commonly known as artificial ageing. Typical artificial ageing temperatures are in the range 150°C to 250°C, and artificial ageing times can be as long as 12 hours. Industrial artificial ageing strategies are designed to produce the optimum size, distribution, type and morphology of strengthening precipitate, and may involve one or more stages at different temperatures, a period of natural ageing prior to artificial ageing, or an intermediate ageing treatment at lower temperature (usually 60-120°C) known as "preageing" prior to artificial ageing.

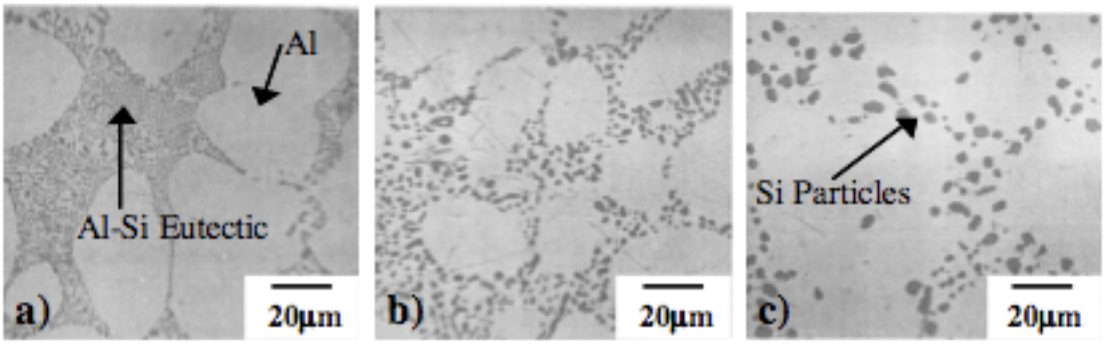

Figure 2.5- *Morphological evolution of eutectic silicon in A356 aluminium alloy during solution treatment at 540°C; (a) as-cast, (b) 2 hours, (c) 8 hours, [26].*

2.2.3 Precipitation Strengthening Mechanism

The strengthening effect of precipitation is related to the interaction of glide of dislocation with the precipitated particles, which act as obstacles to dislocation movement. It is dependent on several factors including: the particle characteristics (i.e. size, shape and volume fraction), their distribution within the matrix, and the nature of the particle-matrix interface. The strength contributions from atoms in solid solution and from shearable and non-shearable precipitates change during ageing, while contributions from lattice, dislocations and grain boundaries are constant. Typically the dislocations pass the precipitate using the most energetically favourable method available. In general there are only two types of interaction: particle cutting in the case where the particle is shareable, and dislocation-looping around unsherable particles. Moving dislocations can shear small and not too hard precipitates (Figure 2.6 - a). Larger and harder precipitate cannot be sheared by the moving dislocations that more likely pass the precipitates by bowing, leaving a dislocation ring

around the precipitate (Figure 2.6 - b). Figure 2.6 - c shows the different strength contributions to the total yield strength for different ageing time.

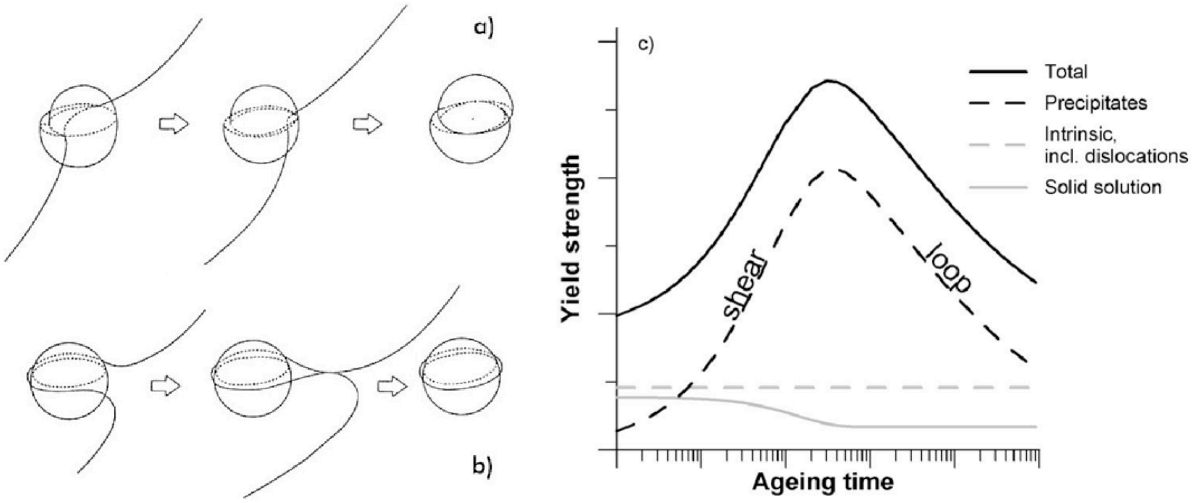

Figure 2.6 - *Dislocations passing mechanism, a) shearing, b) looping. Different strength contributions to the total yield strength [24]*

As long the precipitates can be sheared, the alloy's yield strength increase with increasing radius of the precipitates. On the contrary, when dislocations pass the precipitates by looping, the alloy's yield strength decrease with increasing size of the precipitates [24]. Long time and/ or too elevated temperature annealing exposure can results in overaging. It consists in coarsening of second phases used for strengthening age-or precipitation hardenable alloys.

2.3 Ni and V trace elements

2.3.1 The issue of Ni and V trace elements

Trace elements may often be present in aluminium alloys, either as impurities or by design, and can have both beneficial and adverse effects on the microstructure. Impurity issues in primary Aluminium smelting have historically been focused on the control of particles and dissolved hydrogen and alkali earth metals. However, an emerging problem is the increase in certain impurities, such as Ni and V. Both of them come principally from the anodes of the Hall-Héroult electrolytic process, but in the case of the Vanadium, a small contribution is given by the Alumina [1]. Considering the decrease in quality of petroleum coke observed in recent years, trace elements

and metal impurities are expected to rise in the future with significant implications for the ability of cast houses to meet customers' chemical specifications (Figure 2.7).

It is reported that the Ni and V content in the coke will enrich concentrations of 420 and 1080 ppm, respectively [27]. Currently, there is no cost effective or efficient method available for the removal of these impurities, and the response to the problem is mainly monitoring the V and Ni levels and checking for any negative influence [1].

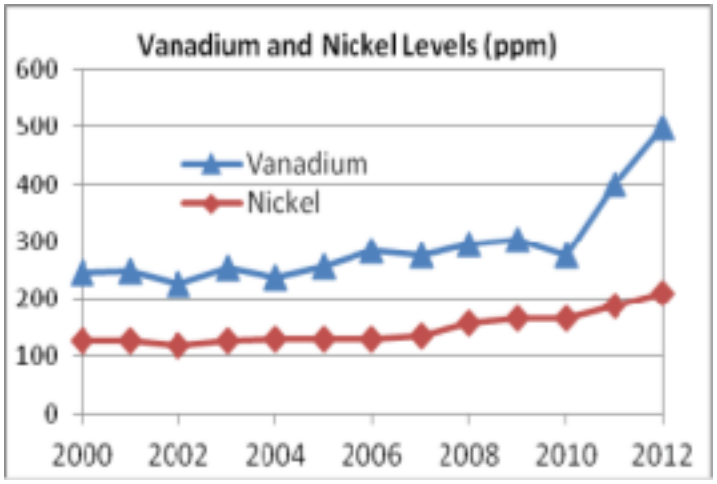

Figure 2.7 - *V and Ni Level in Petroleum Coke [2.27].*

2.3.2 The influence of Ni addition in Al-Si Alloys

Nickel has a low distribution coefficient ($K_d = C_s/C_l$), and it is reported that it remains in the liquid until the later stages of solidification. In commercial Al-Si alloys, where Fe is present as an impurity, Ni is more likely to be associated with iron, i.e. in AlFeSi intermetallics and eventually segregate at the grain boundaries, than be dissolved in the α-Al matrix.

There is a lack of information about the Ni additions below 1000 ppm in the Al-Si foundry alloys. Grandfield et al [28] studied the effect Ni and V combined additions of 300 ppm of each in a AA6063 and A356 alloys. In the as-cast condition, the Ni was mainly found in the intermetallic phase, the π-$Al_8Mg_3FeSi_6$ in an AlSiNi phase with unknown stoichiometry. Mechanical Properties were weakly influenced, nevertheless no significant differences were noticed in the corrosion.

Zhu *et al*. [29] evaluated the influences of Ni addition, varying from 80 ppm to 500 ppm in a A356 alloy, results were in concordance with the work conducted by Grandfield et al., though an identified AlSiFeNi phase was detected.

Moreover, as documented by Garci [30], brittle Al_3Ni particles were detected in Al-7wt%Si alloy containing 0.5 and 0.1 wt% of Ni. These particles exercised a negative effect on the tensile properties, decreasing strength, elongation and hardness.

T.H.Ludwig *et al*. [31] studied the influence of Ni addition in both high purity binary Al-7wt%Si and commercial purity A356 foundry alloys. Ni addition, over 300 ppm, resulted in the formation of the two Al_3Ni and Al_9FeNi intermetallic phases. The first one was fine and distributed in the immediate vicinity of the eutectic Si crystals in both the alloys, while the second one occurred in the commercial alloys, forming distinct script or oval shape particles in the proximity of the π-$Al_8Mg_3FeSi_6$ phase.

In another work [32] the high temperature strength of Al-7wt%Si and Al-12wt%Si was investigated. The as-cast microstructure consisted of a network of interconnected Si lamellae and 3D shape Ni-rich intermetallics. After the solution heat treatment, the stability of the Si-eutectic network was stabilized by the Ni-rich intermetallics that maintain their contiguity to the spherodized Si particles. As a result the high temperature strength at 250°C and, in particular, the yield strength is evidently enhanced. The optimal concentration was established at 1wt%.

In the end, D.Casari *et al.* [2] reported that Ni addition of 0.06 wt% strongly influenced the tensile properties of the sand cast A356 alloy in as-cast condition, leading to a reduction of both the Yield Strength and Ultimate Tensile Strength by 87% and 37%, respectively. Ni-rich intermetallic where observed in the fracture surface, prone to fracture more easily than other secondary phases.

2.3.3 The influence of V impurities in Al-Si Alloys

V is a slow diffusing peritectic element, showing the maximum solubility (~ 0.4 wt%) at the peritectic temperature of 611°C [33]. In most cases V resides in the Al matrix [34] whereas V containing intermetallic particles are unlikely to form below the concentration of 0.1wt%. Is reported by Mondolfo [35] that V, and in particular the peritectic precipitation of Al_3V, had some beneficial effect on the grain refinement, even thought it was less efficient than Ti and/or B. Additionally, the presence of 0.2 wt% V in a high purity alloy Al-7Si-0.3Fe (2.18) facilitated the precipitation of Fe-rich phases as a fine scale Chinese script, otherwise in the absence of V as an alloying element the Fe-rich phases exhibited the platelets shape. Grandfield et al. (2.9) evaluated the influence of 0.03wt% V addition in both AA6063 and A356 alloys, showing a very moderate effect on the tensile properties.

Further investigations on A356 alloy in the as-cast condition [1] revealed an increase in strength, due to the solid solution strengthening effect produced by the addition of 0.1wt% V.
Accordingly, a significant improvement of tensile strength was achieved in V- and Zr-containing Al-7Si-1Cu-0.5Mg-0.1 Ti foundry alloy [36]. The positive effect was associated with the precipitation of nano-sized trialuminide precipitates, uniformly distributed in the Al-matrix.
As stated by T.H. Ludwig [37], increasing the V content from 0.06 wt% to 0.8wt% in a A356 foundry alloy resulted in a shift of nucleation, minimum and growth temperature of the α-Al by up to 4.5K, whereas the undercooling was not affected. No influence on the grain refinement was discovered. Polyhedral Si_2V phases were detected beyond the concentration of 0.06 wt%, and the β-Al_5FeSi phases began enriching in V with increasing nominal V addition, with changes in morphology from needle to script like.

2.4 Hot Tensile Test

At high temperatures, the procedures and specimens of the tensile test are basically the same as room temperature testing. The key differences are the heating apparatus and specially the design of instruments for measuring strain at high temperature. General characteristics of the high-temperature mechanical test setup, used in this work are given in the following section (Chapter 3, paragh.2).
Metallic materials mechanical behaviour is strongly susceptible to temperature. As temperature increases, the strength of a material usually decreases and the ductility increases. The general reduction in strength and increase in ductility of metals at high temperatures can be related to the effect of temperature on deformation of the material. At room temperature, plastic deformation occurs when dislocations in the material slip. The dislocations can also interblock and build-up in the material as they slip. This build-up of dislocations restricts the slip, and, consequently, the forces necessary to continuing the formation increase. This process is known as strain hardening or work hardening. At elevated temperatures, dislocation climb is another deformation mechanism. Further, the build-up of strain energy from strain hardening can be relieved at high temperatures when crystal imperfections are rearranged or eliminated into new configurations. This process is known as recovery. A more rapid restoration process is recrystallization, in which new, dislocation-free crystals nucleate and grow at the expense of original grains. The restoration processes can be greatly enhanced by the increase in the thermal activity and mobility of atoms at higher temperatures. Thus, lower stress is required for deformation, as shown in the stress-strain diagrams

of several materials at elevated temperatures (Figure 2.8). Another effect that can be accelerated during high temperature testing is strain aging. In the strain aging the loss in ductility can be ascribed to precipitation and diffusion-controlled particle growth along the slip planes [38]. At High temperature, as in the Room temperature case, the choice of the strain rate or cross-head speed is of great importance, because the mechanical properties are strongly influence by this parameter. Several combinations of strain at room temperature can be performed in order to study a multitude of conditions (Figure 2.9).

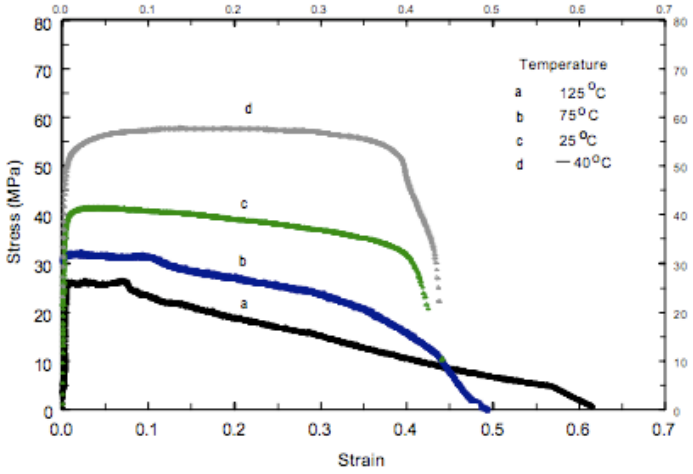

Figure 2.8 - *Typical stress-strain curves at a constant strain rate of 2.78 × 10^3 s^{-1} showing effect of different temperatures [39].*

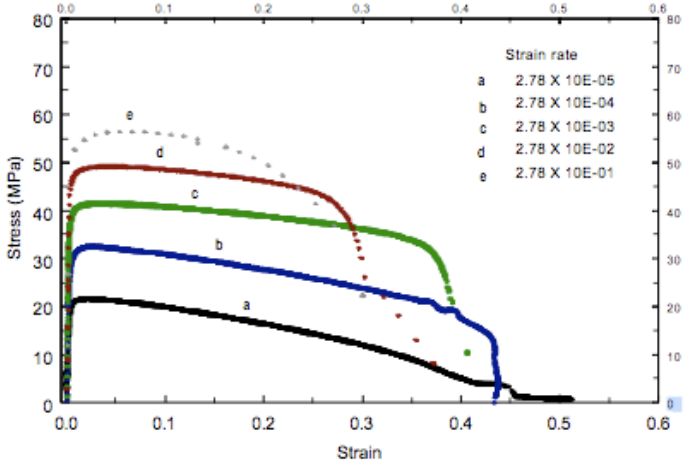

Figure 2.9 - *Typical stress-strain curves at a constant temperature of 25° C showing effect of different strain rates [39].*

3 Experimental Method

3.1 Alloy Preparation

In this study a A356 hypoeutectic Al-Si foundry alloy, was used as the base alloy.According to previous work [2], as received, ingots were melted in charges of 16 kg each in a boron-nitride coated clay-graphite crucible. Trace elements were added in concentrations of 600 and 1000 ppm of Ni and V, respectively. In order to avoid any masking effect or interactions with additional elements, neither Sr nor Na were added as modifier agents. The melting temperature was monitored with the Alspeck-H probe and was kept constant at 740°C ± 5° C. Samples from the three different melts were taken throughout the casting trials and were analysed by optical emission spectroscopy (OES). The chemical compositions of the reference alloy A356 and the Ni- or V-containing alloys are given in the Table 3.1

Table 3.1. - *Chemical composition (wt %) of A356 reference alloy and Ni/V- contaminated alloys as measured by OES.*

Alloy	Addition (ppm)	Si	Fe	Mg	Ni	V	Al
A356	-	7.054	0.092	0.355	0.003	0.007	bal.
A356 + Ni	600	6.902	0.087	0.344	0.061	0.007	bal.
A356 + V	1000	6.992	0.094	0.349	0.003	0.108	bal.

The content of Hydrogen in the melts was measured in-situ using the Alspek- H probe. Melts were degassed with argon gas in order to obtain a hydrogen concentration of 0.08 mlH_2/ 100 gAl. The alloys were then poured in both sand and steel moulds.

3.2 Casting and Heat Treatment

After the melt preparation the alloys were poured in both sand and steel moulds.

Sand castings were obatained using the tensile testing bars propoused by [Daniele, Dispinar and Campbell]. The bar shape varied from cylindrical to tapered, with diameter increasing gradually from 15 mm at the bottom and 20 mm at the top.The cooling rate in the middle of the sand-cast specimen was 1.3 K/s.A L-shaped steel mould was chosen for the permanent mould castings.UNI 3039 specfification was considered. The temperature of the die was kept at a temperature of 300° C during the casting trials. The cooling rate in the middle of the permanent mould-cast specimen was 4.2 K/s.Part of the samples originating from both the casting were subjected to a T6 heat treatment.

They were solutionaized at 540° C for 4 hours, quenched in a water bath at 20°C, and finally aged at 160°C for 6 hours.Twelve different experimental conditions were investigated (Table 3.2), and at least five specimen were tested for each condition.

Table 3.2 - *Specimens condition specification, specimens testing sequence.*

Alloy	Mould	Condition	Alloy Code	Testing sequence
A356	Sand	as-cast	A356-AC	01;07;13;19;25
		T6	A356-T6	02;08;14;20;26
A356 + 600 ppm Ni	Sand	as-cast	N-AC	03;09;13;21;27
		T6	N-T6	04;10;14;22;28
A356 + 1000 ppm V	Sand	as-cast	V-AC	05;11;15;23;29
		T6	V-T6	06;12;16;24;30
A356a	Permanent Mould	as-cast	A356 PM-AC	31;37;43;49;55
		T6	A356 PM-T6	32;38;44;50;56
A356 + 600 ppm Ni	Permanent Mould	as-cast	N PM-AC	35;41;47;53;59
		T6	N PM-T6	36;42;48;54;60
A356 + 1000 ppm V	Permanent Mould	as-cast	V PM-AC	33;39;45;51;57
		T6	V PM-T6	34;40;46;52;58

3.3 Specimen

In accordance with the normative UNI EN ISO 689202, cylindrical specimen reported in Figure 3.1 was chosen.

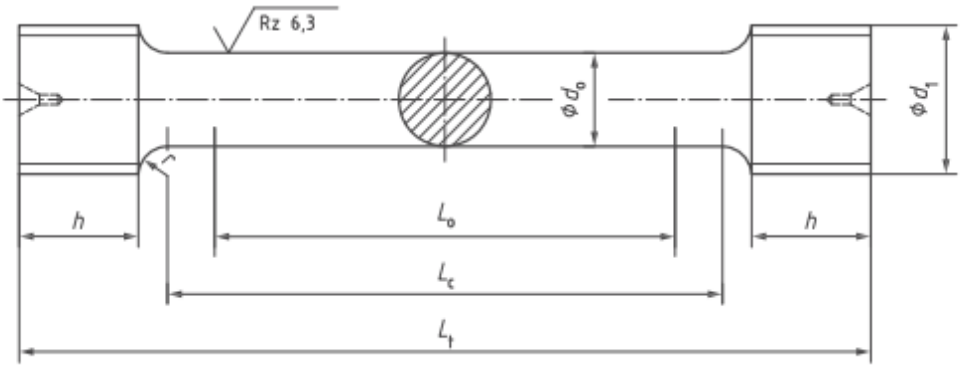

Figure 3.1- *Example of cylindrical tensile test machined specimen, UNI EN ISO 689202.*

The specimen has enlarged ends,15 mm long,for gripping. The cross-sectional diameter, d_0, is 6 mm.The gauge length, L_0, is 30 mm. The total specimen length, L_t is 135 mm.

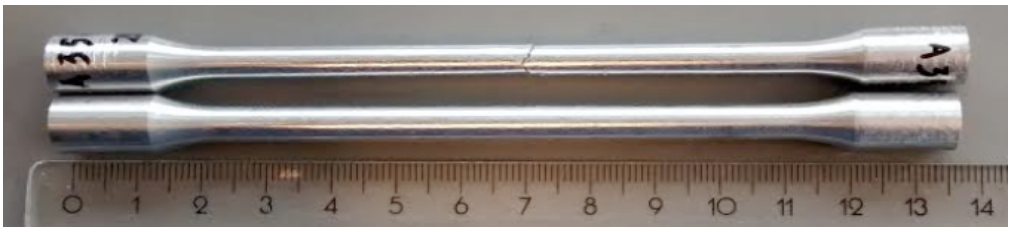

Figure 3.2- *Tensile specimen before and after the Hot Tensile Test.*

3.4 Hot Tensile Test

High temperature tensile tests were performed on MTS 880 universal testing machine (10 tons) equipped with a 250°C furnace chamber and a MTS Teststar control units (Figure 3.3). In order to ensure that errors that might occur during the experimental procedure, such as mounting time variation, specimens slipping from the grip, errors in the software settings, affect all the classes with the same probability, samples were tested in successive order among each category (Table 3.1). Considering the main purpose of this work, which is to study the effects of trace elments in the base alloy on the tensile behavior at elevated temperature, all the specimens were tested at the same temperature, 235±5 °C.

The crosshead speed was 1mm/min and the applied load was restricted to 40 kN.The following steps describe the standardized procedure.The first step consisted in heating the furnace chamber by setting the maximum temperature's value at 250°C. Starting from room temperature, one hour was necessary to reach the reference temperature of 247 ± 3°C.

Figure 3.3 – *MTS 880 tensile testing machine equipped with a furnace chamber positioned around the specimen.*

Once the reference temperature was attained, the chamber was opened and the mounting phase took place (7 minutes), the temperature decreased from 247 ± 3°C to 100±5°C. Subsequently,an other 12 minutes were needed to re-establish the reference temperature. To ensure the stability of the temperature in the entire specimen, it was exposed another 3 minutes, in which time the accuracy of the constant temperature was checked on the display of the furnace device. After a total time of 15 min, the test started. One specimen was used to a direct temperature investigation utilizing a thermocouple. The tip of the thermocouple was placed into a 1mm diameter hole centered in the gauge length of the specimen.It is important to take into account the differences between the temperature set in the chamber and the one measured on the specimen, as shown in the Figure 3.4.
A specially designed clip-on axial extensometer in stainless steel connected to an optical position measuring system was used to obtain the stress-strain curves. As a result, the high temperature tensile properties such as yield streght, ultimate tensile strenght and elongation, $Rp_{0,2}$, UTS and A%, respectively, were determinated.Specimens before and after the Hot Tensile Test are shown in Figure 3.2.

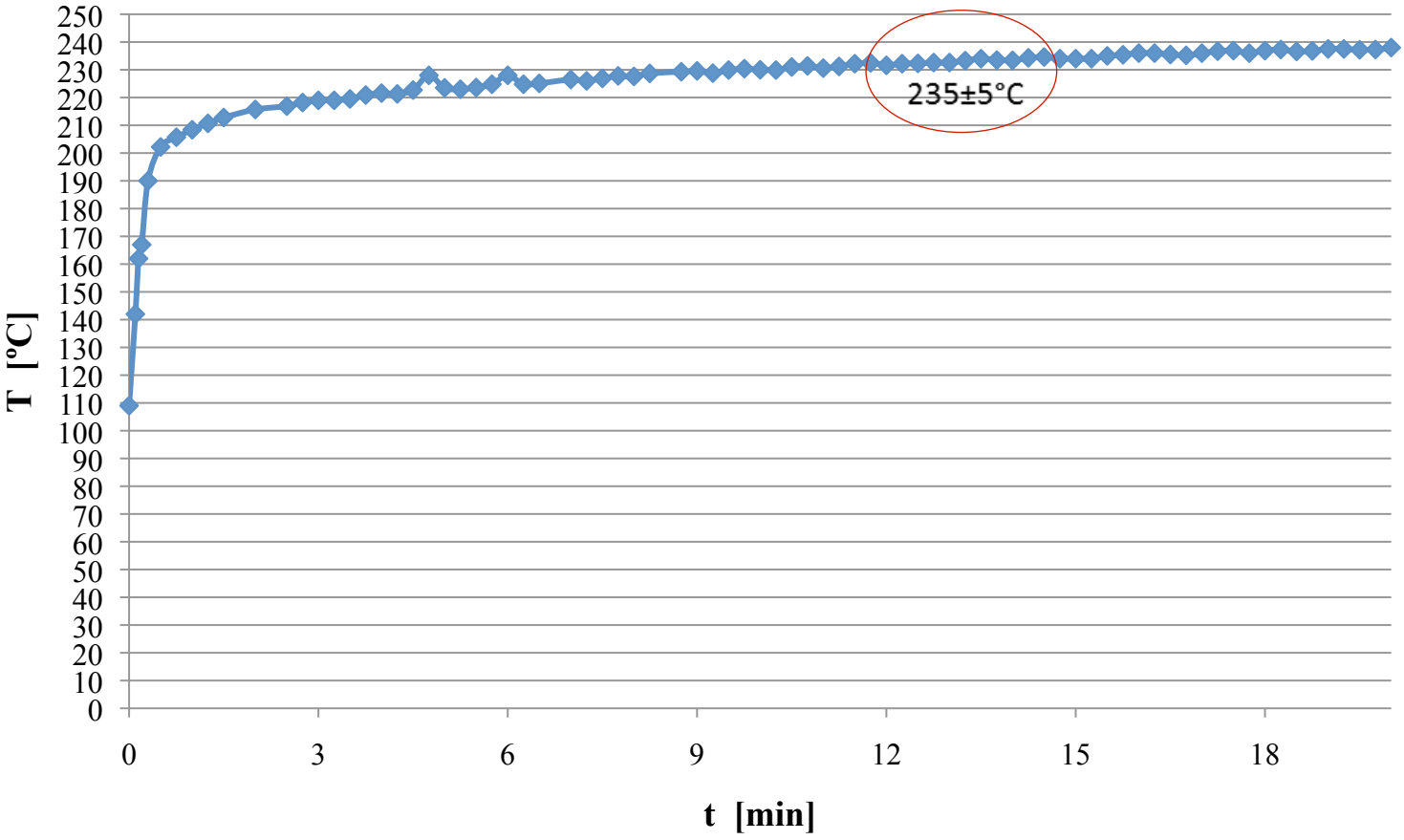

Figure 3.4 – *Temperature measurement conducted by a thermocouple centered in the gauge length of the specimen. 12 min. were necessary to achieve the reference temperature; other 3 min. were needed to stabilize the temperature, after total 15 min. the test started.*

3.4 Microstructure Analysis

After the hot tensile test, the specimens were prepared for microscopy analysis. Samples for the fractographic investigation were sectioned parallel to the fracture surface. Ultrasonic cleaning was used to remove debris, dirt and oil coatings from thefracture surface (Figure 3.5-a). Samples for metallographic investigation were sectioned perpendicular to the fracture surface; they were then embedded in a low-viscosity epoxy resin (Figure 3.5-b). The grinding procedure was performed using SiC papers, from 320 up to 2400, with 15N force for 60 seconds. The samples were then polished on MD-Mol (3µm) at 15 N for 6 minutes and on MD-Nap (1 µm) at 15 N for 6 minutes.Microstructures and fracture surfaces were finally analysed with a HITACHI SU-6600 field emission scanning microscope (FE-SEM) equipped with energy dispersive X-ray spectroscopy (EDS).

Figure 3.5 – *a) Fracture surface sample, b) Fracture profile sample.*

4 Results

4.1 High Temperature Tensile Properties

Tables 4.1 and 4.2 show the average values of the high temperature tensile properties of the reference and Ni/V containing alloys in both sand and permanent moulds conditions.
No significant difference between the reference alloy and the Ni- and V- containig alloys is found betwen the two casting conditions, as shown in the Figures 4.1 and 4.2.
A slight increase in yield strength (Rp_{02}), ultimate tensile strength (UTS) and elongation (A%) can be observed for the permanent mould cast alloys as compared to the sand cast alloys. Additionally, a more uniform distribution of the elongation values (A%) can be noticed for the permanent mould castings. Rp_{02} and UTS have small error bars that indicate the reproducibility and the realibility of the values. In spite of this, A% error bars result are larger.

Table 4.1. – *High temperature tensile properties of the sand cast reference and Ni/V containing alloys.*

Alloy code	Rp_{02} [Map] ± δ	UTS [Mpa] ± δ	A [%] ± δ
A 356 - AC	106,3 ± 3,5	122,2 ± 1,8	2,84 ± 1,07
A 356 - T6	179,7 ± 2,0	185,6 ± 1,8	1,47 ± 1,18
N - AC	102,8 ± 1,8	118,1 ± 3,1	4,26 ± 2,80
N -T6	182,4 ± 5,2	189,3 ± 3,1	1,99 ± 0,83
V - AC	101,4 ± 1,5	118,4 ± 1,9	3,15 ± 0,94
V - T6	177,6 ± 1,4	184,4 ± 1,9	2,08 ± 1,06

Table 4.2. – *High temperature tensile properties of the permanent mould cast reference and Ni/V containing alloys.*

Alloy code	Rp_{02} [MPa] ± δ	UTS [Mpa] ± δ	A [%] ± δ
A 356 PM - AC	109,6 ± 3,3	133,2 ± 4,8	3,93 ± 1,01
A 356 PM - T6	185, 7 ± 4,0	195 ± 3,5	3,90 ± 1,78
N PM - AC	117,2 ± 7, 2	135,8 ± 6,5	2,72 ± 0,79
N PM -T6	186,0 ± 2,5	196,8 ± 2,5	4,08 ± 1,99
V PM - AC	111, 3 ± 5,8	135,5 ± 7,0	3,81 ± 2,38
V PM - T6	192,6 ± 4,7	202,5 ± 4,6	4,65 ± 2,14

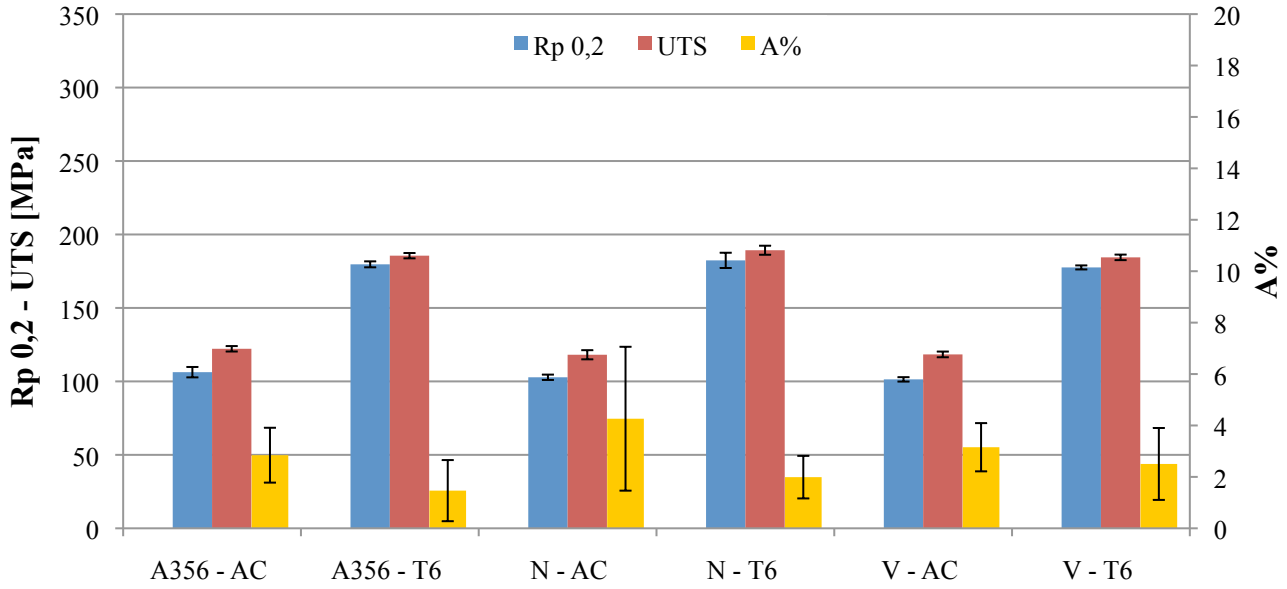

Figure 4.1– *High temperature tensile properties of the sand cast reference and Ni/V containing alloys in as-cast and T6 conditions.*

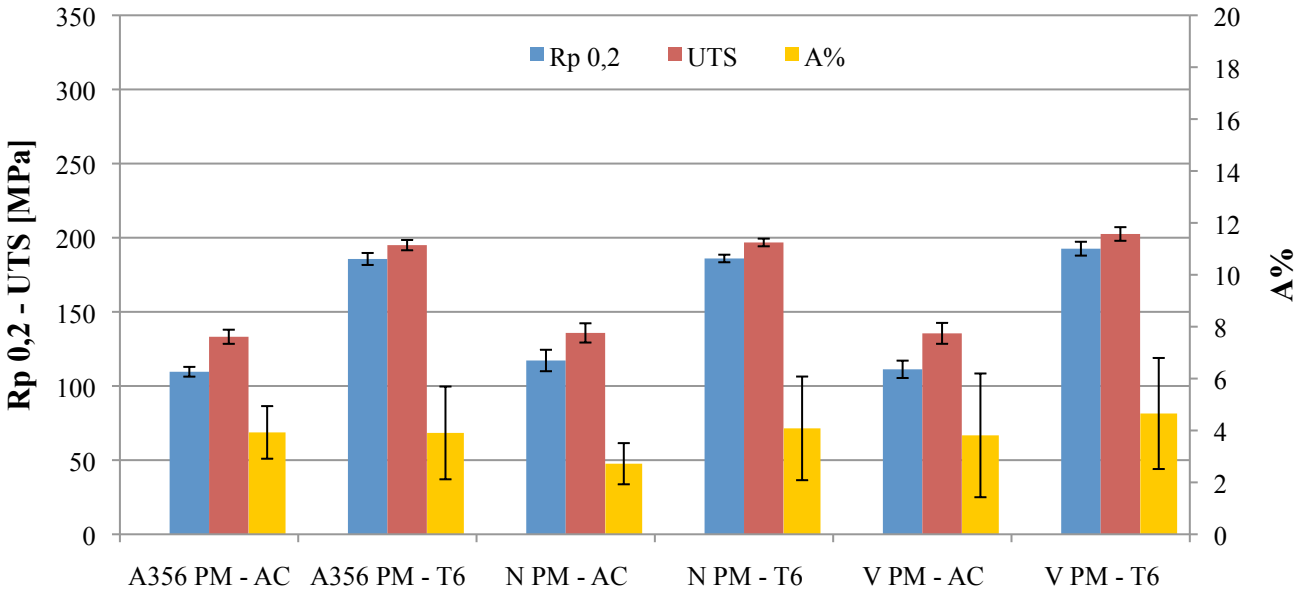

Figure 4.2–*High temperature tensile properties of the permanent mould cast reference and Ni/V containing alloys in as-cast and T6 conditions.*

4.2 Room Temperature Tensile properties versus High Temperature Tensile Properties

Room Temperature Tensile properties of the investigated alloys were evaluated by [D.Casari]. The experimental work revealed that Ni and V strongly affected the mechanical properties of sand cast samples in the as cast condition; brittle Ni-rich intermetallic compounds were detected in the Ni-containing alloy, decreasing the strength, whereas solid solution strengthening of the α-Al matrix was observed in the V- containing. Furthermore, it was noticed that T6 heat treatment and the high cooling rate, due to the permanent mould casting process, could neutralise the detrimental influence of Ni. On the contrary V trace addictions were found to be beneficial for the tensile properties.
The result of both Room and High temperature tensile tests are summarised in Tables 4.3, 4.4, 4.5, 4.6 and reported in Figures 4.3, 4.4, 4.5, 4.6.

The conditions which were compared are mentioned as follows and further, a description of each condition is presented.

1. sand mould as-cast
2. sand mould T6
3. permanent mould as-cast
4. permanent mould T6

1. Reference and Ni-containing sand cast samples in the as-cast condition show a significant increase in the yield strength (Rp_{02}) by 26% and 138% respectively, at High temperature as compared to the Room temperature (A356-AC RT and HT, N-AC RT and HT in Figure 4.3). The difference between the Ni-containing RT vs. HT alloys is emphasised by the low strength measured at Room temperature. In contrast, a small decrease in both Rp_{02} and UTS, by 11% and 26% respectively, can be observed for the V contang alloys at High temperature as compared to the Room temperature (V-AC RT and HT in Figure 4.3).All the alloys exhibit a relevant increase of A% values at 235°C.
2. Considering the sand cast heat treated alloys, a small decrease in strength at High temperature is visible, as shown in the Figure 4.3. The Ni- and V-containing samples were more affected showing a decrease of the yield and ultimate tensile strength by 14% - 22% and 18% - 26% respectively (N-T6 RT and HT, V-T6 RT and HT in Figure 4.3).

Table 4.3 – *Room temperature and High temperature tensile properties of the sand cast reference and Ni/V containing alloys in the as-cast condition.*

Alloy code	Rp 0,2 [Mpa]±δ	UTS [Mpa] ±δ	A [%] ±δ
A356-AC RT	80,7 ± 10,4	128,4 ± 8,0	1,46 ± 0,53
A356-AC HT	106,3 ± 3,5	122,2 ± 1,8	2,84 ± 1,07
N-AC RT	43,2 ± 6,0	93,8 ± 9,1	1,73 ± 0,28
N-AC HT	102,8 ± 1,8	118,1 ±3,1	4,26 ± 2,80
V-AC RT	114,5 ± 4,7	160,5 ±10,0	1,33 ± 0,45
V-AC HT	101,4 ± 1,5	118,4 ± 1,9	3,15 ± 0,94

Table 4.4 – *Room temperature and High temperature tensile properties of the sand cast reference and Ni/V containing alloys in the T6 condition.*

Alloy code	Rp 0,2 [Mpa]±δ	UTS [Mpa] ±δ	A [%] ±δ
A356-T6 RT	183,2 ± 14,0	212,0 ± 30,1	0,99 ± 0,67
A356-T6 HT	179,7 ± 2,0	18562 ± 1,8	1,47 ± 1,19
N-T6 RT	212,7± 31,3	244,6 ± 30,6	0,90 ± 0,35
N-T6 HT	182,4 ± 5,2	189,3 ± 3,1	1,99 ± 0,83
V-T6 RT	216,9 ±7,9	250,4 ± 8,8	1,14 ± 0,59
V-T6 HT	177,6 ± 1,4	184,4 ± 1,9	2,50 ± 1,39

Table 4.5 – *Room temperature and High temperature tensile properties of the permanent mould cast reference and Ni/V containing alloys in the as-cast condition.*

Alloy code	Rp 0,2 [Mpa]±δ	UTS [Mpa] ±δ	A [%] ±δ
A356 PM AC-RT	93,4 ± 4,8	172,8 ± 7,0	4,0 ± 0,75
A356 PM AC-HT	109,6 ± 3,3	133,2 ± 4,8	3,93 ± 1,01
N PM AC-RT	93,4± 5,5	169,1 ± 9,9	3,44 ±1,32
N PM AC-HT	117,2 ± 7,2	135,8 ±6,5	2,72 ± 0,79
V PM AC-RT	91,6 ± 4,0	171,1 ± 10,4	3,54 ± 1,12
V PM AC-HT	111,3 ± 5,8	135,5 ± 7,0	3,82 ± 2,39

Table 4.6– *Room temperature and High temperature tensile properties of the permanent mould cast reference and Ni/V containing alloys in the T6 condition.*

Alloy code	Rp 0,2 [Mpa]±δ	UTS [Mpa] ±δ	A [%] ±δ
A356 PM T6-RT	224,3 ± 2,0	282,2 ± 6,9	3,22 ± 0,84
A356 PM T6-HT	185,6 ± 4,0	191,4 ± 7,7	3,90 ± 1,79
N PM T6-RT	228,7± 3,1	284,8 ± 7,4	3,25 ± 1,21
N PM T6-HT	186 ± 2,5	196,8 ± 2,6	4,08 ± 2,0
V PM T6- RT	224,2 ± 1,5	289,5 ± 8,6	3,60 ± 1,50
V PM T6-HT	192,6 ± 4,7	202,5 ± 4,6	4,65 ± 2,14

3. Similar trends can be observed in permanent mould cast alloys. All the classes in the as-cast condition show an increase in the yield strength at High temperature as compared to Room temperature. However the difference pronounced as in the sand cast alloys. A general reduction of UTS is noted for the samples tested at 235°C.
4. The decrease of strength previously discussed in the heat treated sand mould castings is more significant in the permanent mould castings. UTS drops approximately 20% for each experimental condition as evidenced by Figure 4.6.

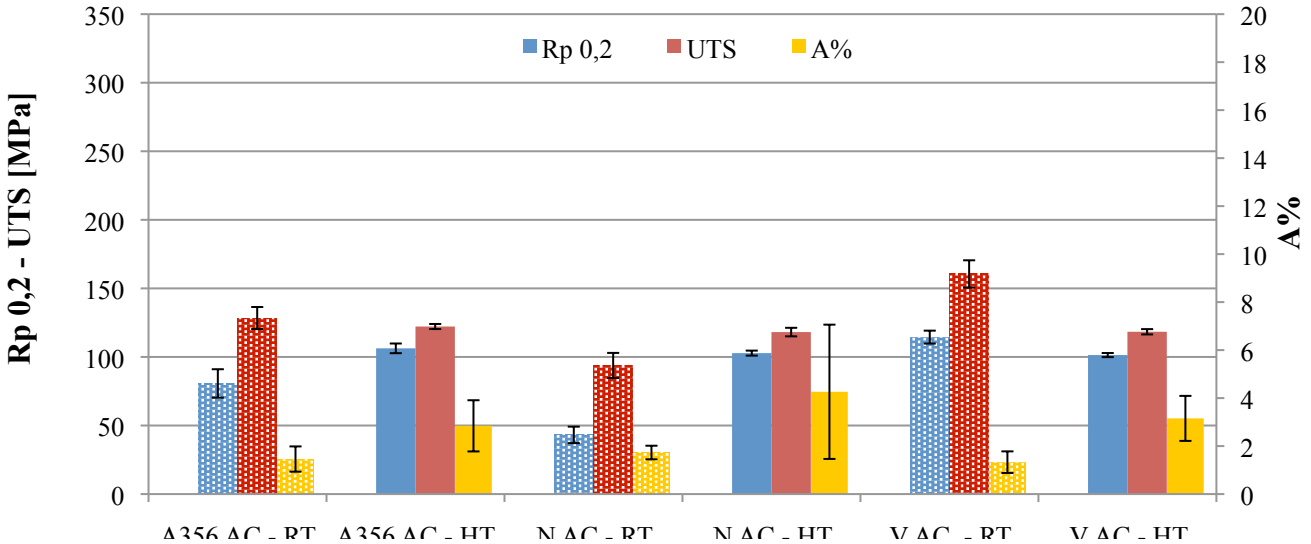

Figure 4.3– *Room temperatures vs High temperature tensile properties of the sand cast reference and Ni/V containing alloys in the as-cast condition.*

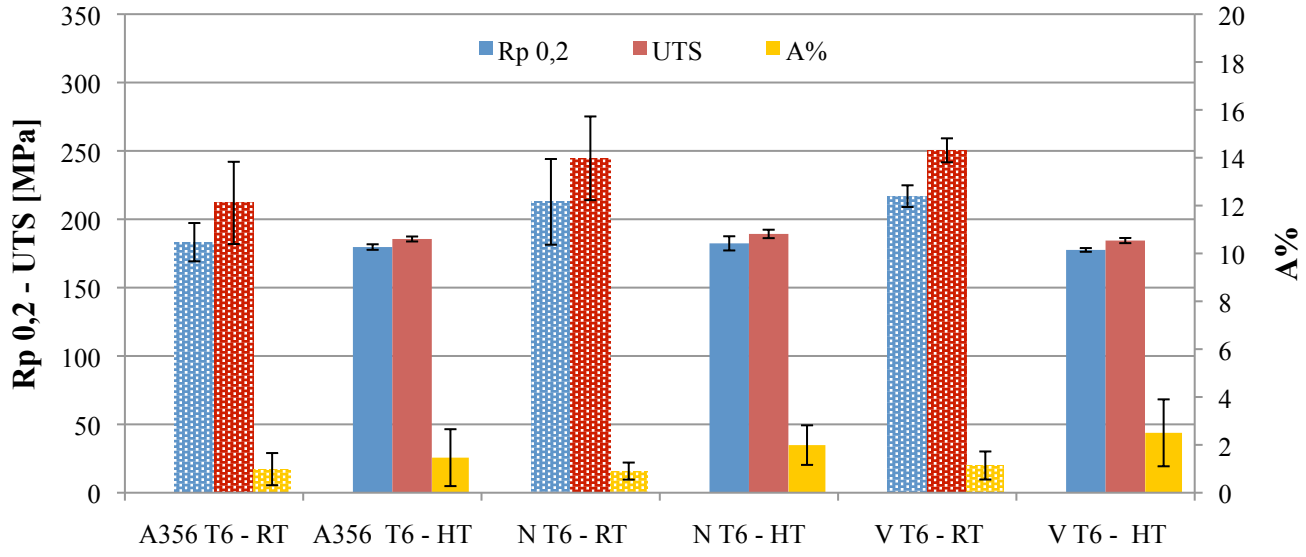

Figure 4.4– *Room temperatures vs High temperature tensile properties of the sand cast reference and Ni/V contaminated alloys in the T6 condition.*

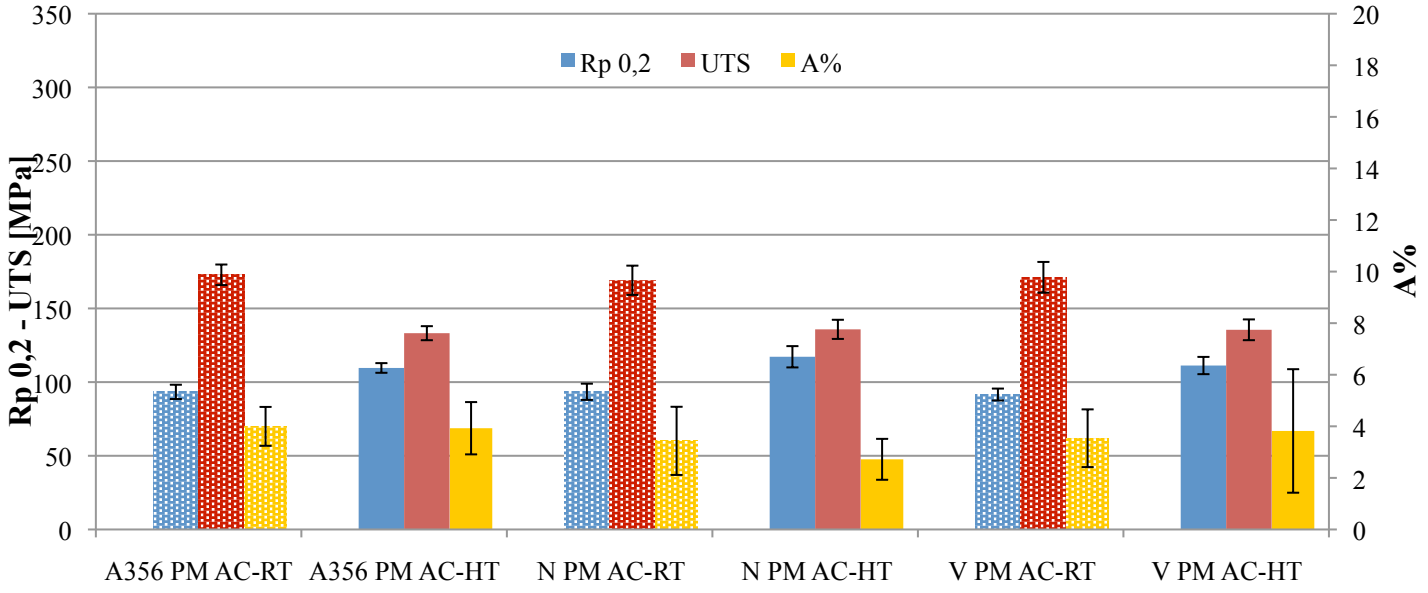

Figure 4.5 – *Room temperatures vs High temperature tensile properties of the permanent mould cast reference and Ni/V containing alloys in the as-cast condition.*

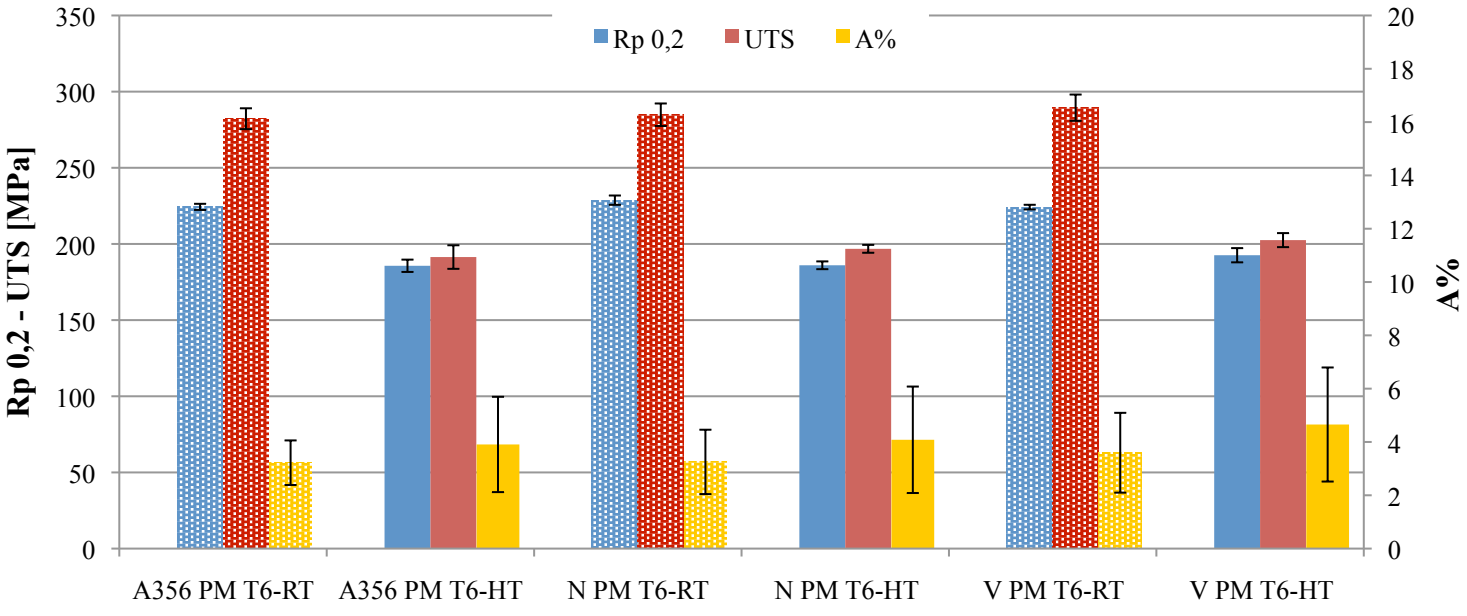

Figure 4.6– *Room temperatures vs High temperature tensile properties of the permanent mould cast reference and Ni/V containing alloys in the T6 condition.*

4.3 Strain Hardening in the as-cast alloys

Stress-Strain curves are presented in Figure 5.1. According to sand cast/permanent cast analogy only the first series of samples was taken into consideration.

Young's Modulus (E) and Strain Hardening Rate (**Θ**), calculated as the slope of the Stress-Strain curves at given strains (true strain= 0.05%; 0.10%; 0.15%; 0.20%; 0.25%; 0.30%) are shown in Figure 5.1 Numerical results are summarised in Table 5.1.

Both Reference and Ni-containing alloys exhibit an increase in strain hardening rate at elevated temperatures. On the other side, the opposite behaviour is noticed in the V-added alloys.

In all the conditions the Young's module at 235°C was lower than the Room Temperature case, about 80 GPa, and 60 GPa respectively.

4.4 Microstructural and Fractographic Investigation.

Microstructural and fractographic investigations were performed analysing the fracture profiles and surfaces of the samples.

Backscattered electron (BSE) images of the reference, Ni- and V-containing alloys in as-cast and T6 heat treated conditions are shown in Figure 4.7. Only the sand cast samples are presented.

The main features are α-Al dendrites and needle-like Al-Si eutectic, Fe-bearing particles such as *π-$Al_8FeMg_3Si_6$* and *β-Al_5FeSi*, *Ni-rich* compounds and *Mg_2Si* particles are also observed.

In the eutectic region platelet-like *β-Al_5FeSi* and *'Chinese Script' π-$Al_8FeMg_3Si_6$* are sometimes associated(Figure 4.7- c). Ni-based intermetallics phases, exhibiting an oval shape, are observed in the sand cast alloy with Ni addiction (Figure 4.7 - c, d).

A slight increase of Fe-rich and Mg_2Si particle amount is observed in the V-containing samples (Figure 4.7 - c, d).

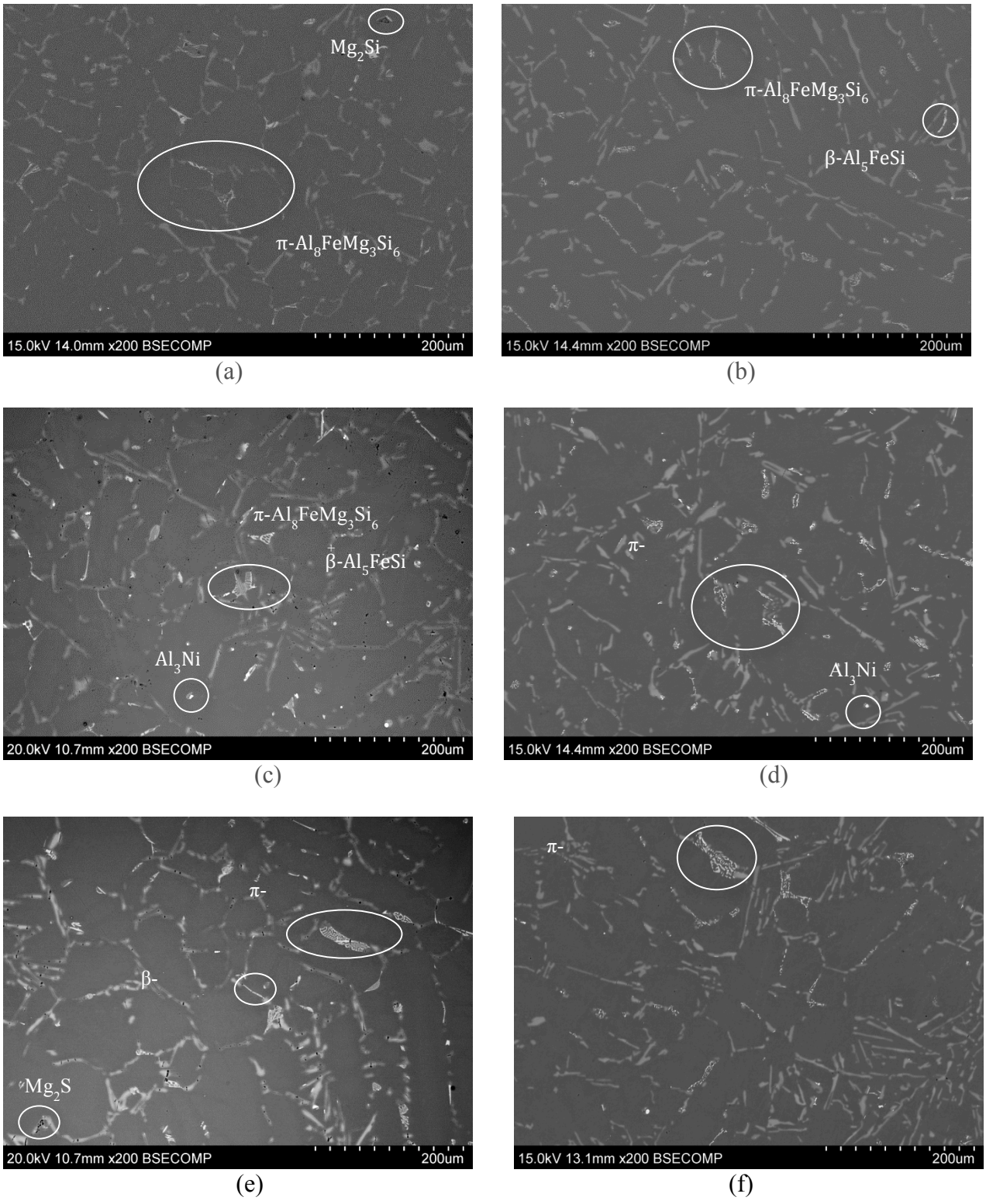

Figure 4.7- *BSE micrographs of sand cast reference and Ni/V- containing alloys in as-cast and T6 conditions tested at high temperature (a) A356-AC, (b) A356-T6,(c) N-AC,(d) N-T6,(e) V-AC, (f) V-T6; Aluminium dendrites are in dark grey, eutectic Si crystal in light opaque grey, π-$Al_8FeMg_3Si_6$ and β-Al_5FeSi in light clear grey,Mg_2Si in black and Ni-rich intermetallics in white.*

A moderate spheroidisation of eutectic Si particle is noted in the T6 heat treatment samples due to solutionising, on the other hand, Fe-bearing compounds have a more marked tendency to spheroidise as visible in Figure 4.7. b, d, f.

Figure 4.9 shows the fracture profile of the reference, Ni- and V-containing alloys in as-cast and T6 heat treated conditions.

It is evident that the fracture path mainly follows the eutectic region as indicated by the arrows in Figure 4.9 - a,b. Below to the main fracture, multiples cracks oriented normally to the applied stress are observed in both Si-particles and Fe-bearing phases (Fig 4.8).

In addition, a significant plastic deformation of Al-dendrites is noticed in all the investigated alloys (Fig 4.9 - c).

No significant difference in the fracture path is observed in heat treated alloys.

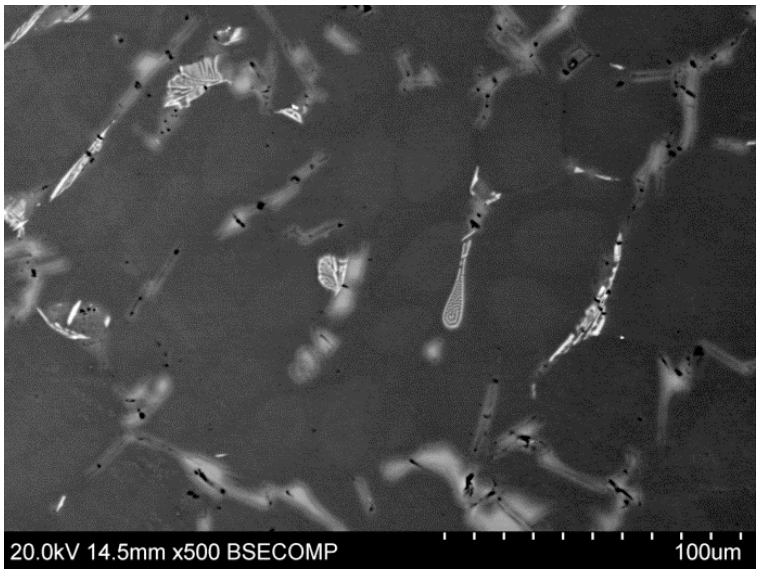

Figure 4.8- *BSE micrograph of the sand cast A356 alloy (as-cast) close to the fracture surface, showing cracked eutectic Si-particles and Fe-bearing compounds.*

SEM micrographs of the fracture surfaces are presented in Figure 4.10.

Sand cast A356 alloys in both as-cast and T6 conditions, exhibit a mixed ductile-brittle fracture as evidenced by the presence of dimples together with quasi-cleaved Si flakes.

In accordance with previous findings [2], Ni-rich intermetallics compounds are detected in a sand cast alloys with 600 ppm Ni (Figure 4.11 a and b).

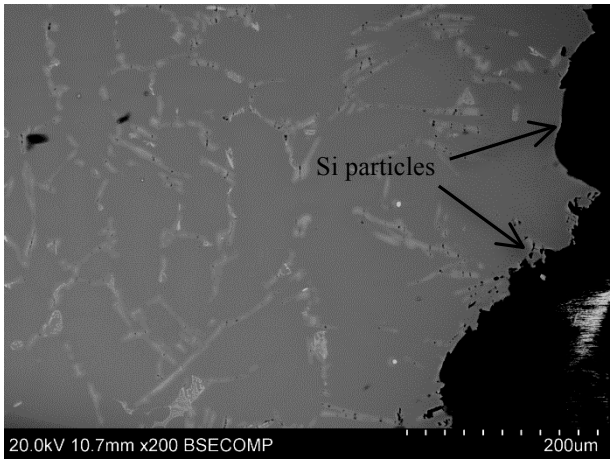

(a)

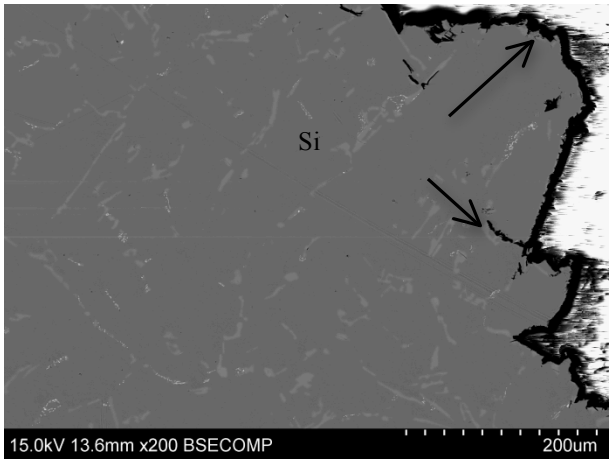

(b)

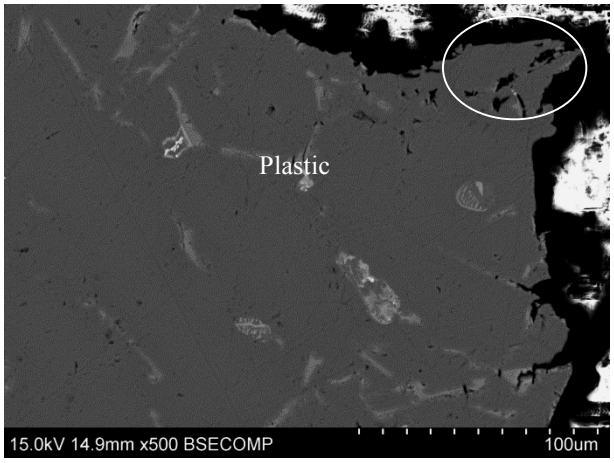

(c)

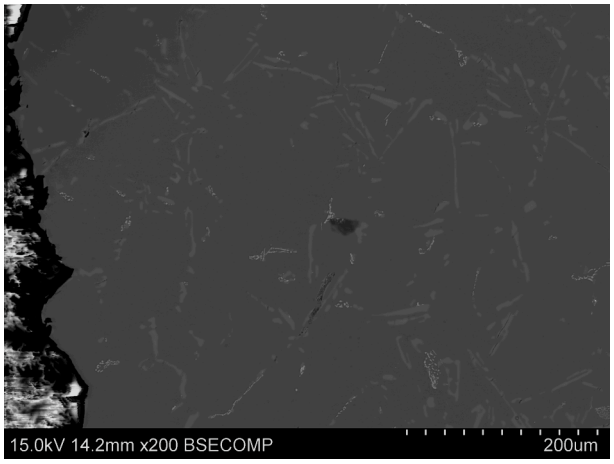

(d)

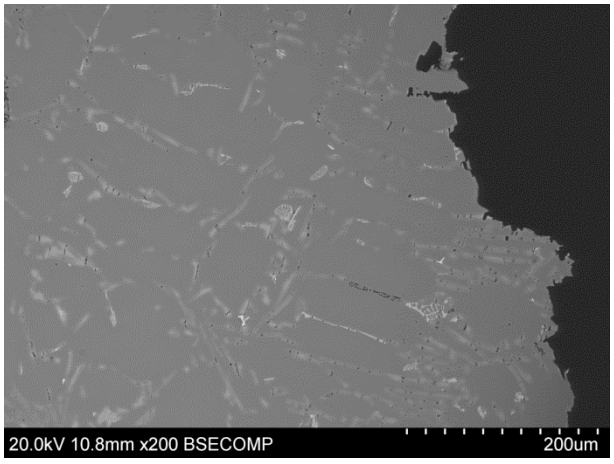

(e)

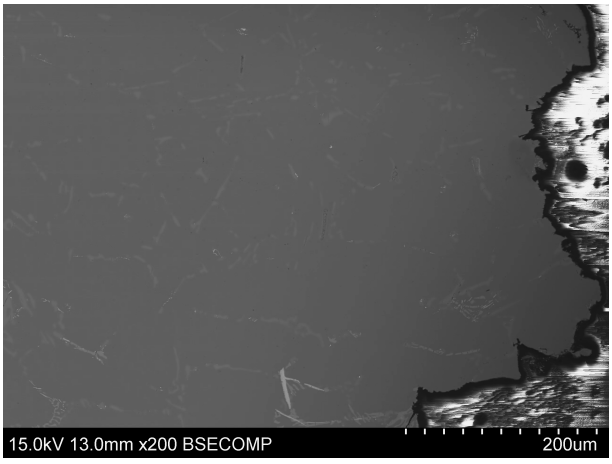

(f)

Figure 4.9- *BSE fracture profiles of sand cast reference and Ni/V- containing alloys in as-cast and T6 conditions : (a) A356-AC, (b) A356-T6,(c) N-AC,(d) N-T6,(e) V-AC, (f) V-T6, A Si-driven quasi-cleavage and matrix crack is the main fracture mode, large plastic deformations can be easily observed. There are no significant differences in crack paths between as-cast and T6 heat treated alloys.*

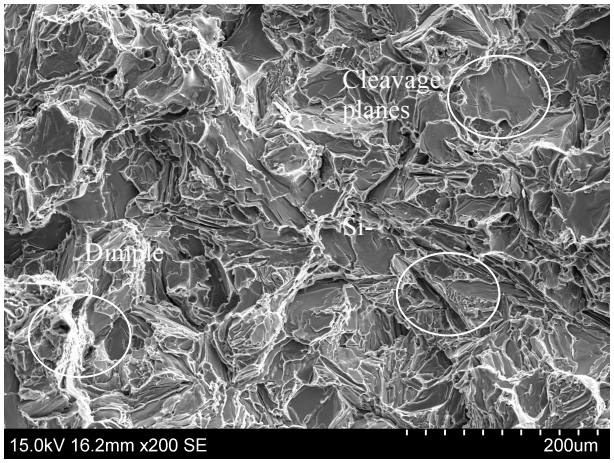

(a)

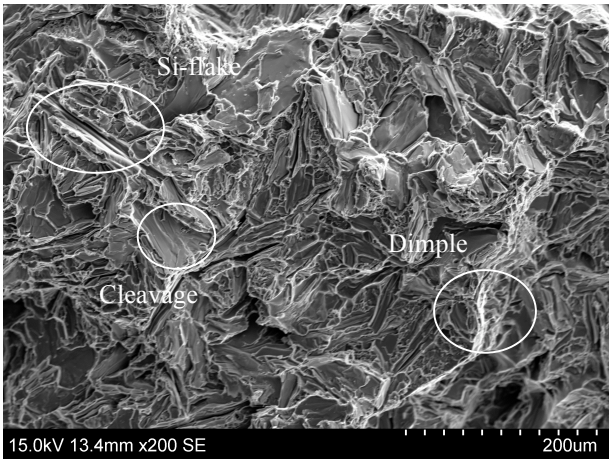

(b)

Figure 4.10- *SEM micrograph of the fracture surface of sand cast A356 reference alloy in as-cast (a) and T6 conditions (b) showing the typical features of mixed ductile-brittle fracture. Si- flakes persist after the T6 heat treatment.*

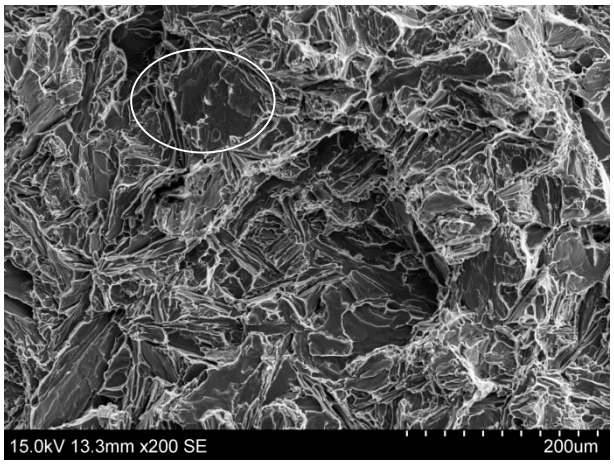

(a)

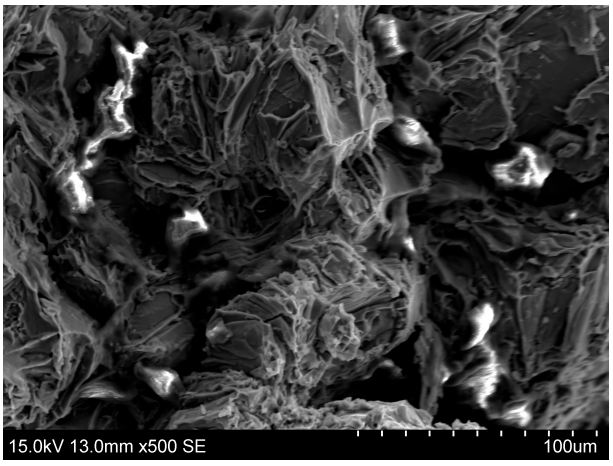

(b)

Figure 4.11- *Ni-rich intermetallics compounds detected in a sand cast alloy with 600 ppm Ni, in the as-cast condition (a),(b).*

5 Discussion

The result will be discussed in three sections. Firstly a general overview of the results obtained will be given. Secondly both the sand cast and the T6 conditions will be analysed.
Finally fracture behaviour will be examined.

5.1 Overview of the results obtained

Tables 4.1, 4.2 and Figures 4.1, 4.2 summarise the high temperature tensile properties of the reference and Ni/V containing alloys in both sand and permanent mould conditions.
In contrast with previous findings [2], the results obtained clearly show that there are no differences between the reference alloy and the Ni- and V- containing alloys. This evidences that neither Ni nor V addition (600 and 1000 ppm respectively) exercises a detrimental effect on the tensile properties. Rp_{02} and UTS have small errors bars that indicate the reproducibility and the reliability of the data whereas A% errors bars result are larger. This is mostly due to the presence of porosity in the cast alloys.

5.2 The as-cast condition and the T6 Condition

5.2.1 Reference and Ni-containing yield strength increase in the as cast condition

Results obtained in the as-cast condition show an unexpected behaviour. It is know that typically tensile properties decrease with increasing temperature. Surprisingly, the sand cast (Figure 4.3) and the permanent mould cast (Figure 4.5) alloys, in the as-cast condition, evidence that the yield strength increases at high temperature as compared to the room temperature. In accordance with what presented in the previous chapter (Chap. 4.2), reference and Ni-containing sand cast samples, A356 AC and N AC show an increase in the yield strength Rp_{02} by 26% and 138% respectively. Similar trends are observed in the permanent mould alloys although the effect is less pronounced.

One possible hypothesis is related to the strain hardening occurring at high temperature. Table 5.1 summarizes the Room temperature vs. High temperature Young's modulus and Strain Hardening Rate (true strain = 0.05%; 0.10%; 0.15%; 0.20%; 0.25% ;0.30%;) of the sand cast reference and Ni/V containing alloys in the as-cast condition. Strain hardening is caused by dislocations

interacting with each other and with barriers which impede their motion through the crystal lattice. Glide of dislocation can be considered a thermally activated process. The rate of strain hardening is derived from the slope of the flow curve. A high rate of strain hardening implies mutual obstruction of dislocation gliding on intersecting system. This can come about (1) through interaction of the stress fields of the dislocations, (2) through interactions which produce sessile locks, and (3) through the interpenetration of one slip system by another which results in the formations of dislocation jogs [40,41]. The basic equation relating flow stress (strain hardening) to structure is:

$$\sigma_0 = \sigma_i + \alpha G b \qquad (1)$$

Figures 5.1-2 a,b clearly show the influence of the high temperature on the strain hardening.
As the test continues the phenomenon is gradually recovered till the point in which the failure takes place and the ultimate tensile strength (UTS) is reached. As the matter of fact Figures 4.3 and 4.4 indicate that as the strain increase, the difference between the high and room temperature curves becomes smaller. The high temperature tensile test does not affect the microstructure, so that, according with the room temperature case, the presence of course flake-like or acicular eutectic Si remain the leader parameter in the failure, which explains the similarities between the room temperature and the high temperature UTS.

Table 5.1- *Room temperature vs. High temperature Young's modulus, E, and Strain Hardening Rate, θ, (true strain = 0.05%; 0.10%; 0.15%; 0.20%; 0.25% ;0.30%;) of the sand cast reference and Ni/V containing alloys in the as-cast condition*

Alloy code	E ± δ	Θ (A= 0,05) ± δ	Θ (A= 0,1) ± δ	Θ (A= 0,15) ± δ	Θ (A= 0,20) ± δ	Θ (A= 0,25) ± δ	Θ (A= 0,30) ± δ
A356-AC RT	75,1 ± 6,2	92,8 ± 29,4	50,8 ± 6,1	49,7 ± 7,4	34,7 ± 4,1	30,4 ± 3,4	26,8± 3,0
A356-AC HT	59,8 ± 3,9	131,5 ± 6,9	59,3 ± 3,7	53,6 ± 2,4	45,2 ± 1,8	38,5 ± 1,4	33,2 ± 1,2
N-AC RT	78,5 ± 6,6	24,4 ± 5,2	24,4 ± 2,5	20,7 ± 1,9	18,1 ± 1,6	16,2 ± 1,4	14,8 ± 1,2
N-AC HT	57,6 ± 4,8	57,8 ± 44,1	57,8 ± 3,6	50,9 ± 2,6	43,3 ± 1,9	37,1 ± 0,7	31,9 ± 0,7
V-AC RT	79,5 ± 8,0	143,1 ± 5,6	70,0 ± 1,8	57,3 ± 1,8	48,5 ± 1,8	41,8 ± 1,6	36,8 ± 1,4
V-AC HT	58,3 ± 3,7	132,0 ± 9,5	58,9 ± 6,2	53,2 ±¯2,4	44,5 ± 1,6	37,6 ± 1,3	32,3 ± 1,0

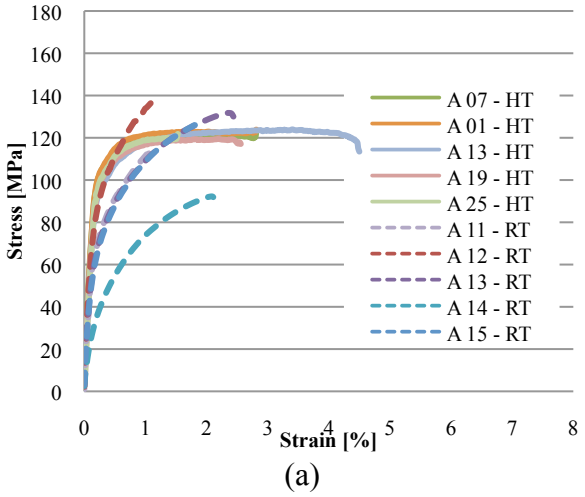

(a)

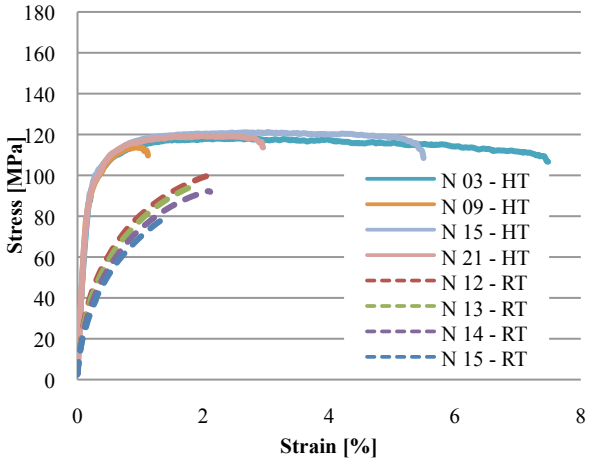

(b)

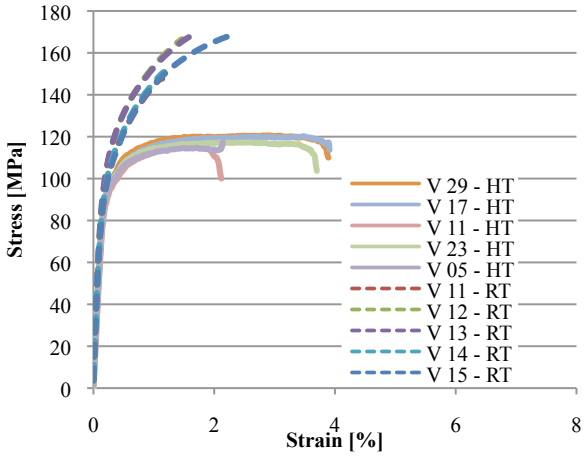

Figure 5.1 –*Comparison between the Stress-Strain curves at Room temperature and High temperature of (a)A356 reference,(b)Ni-containing (c) V-containing sand cast alloys in the as-cast condition. RT and HT in solid and dotted lines respectively.*

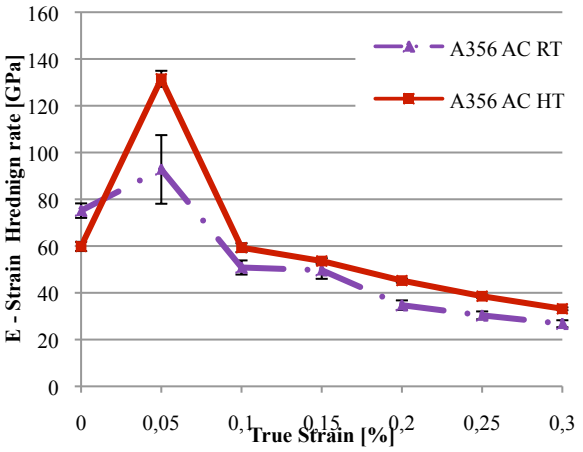

(a)

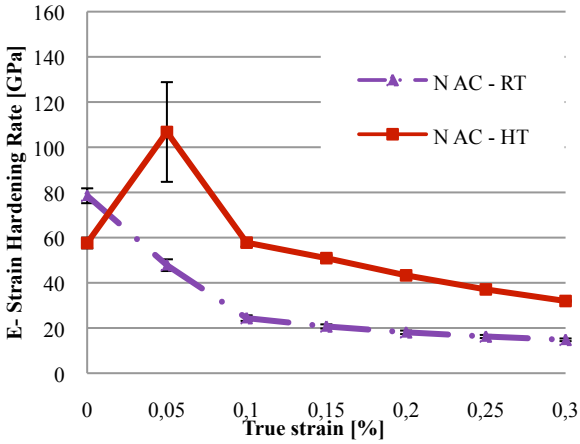

(b)

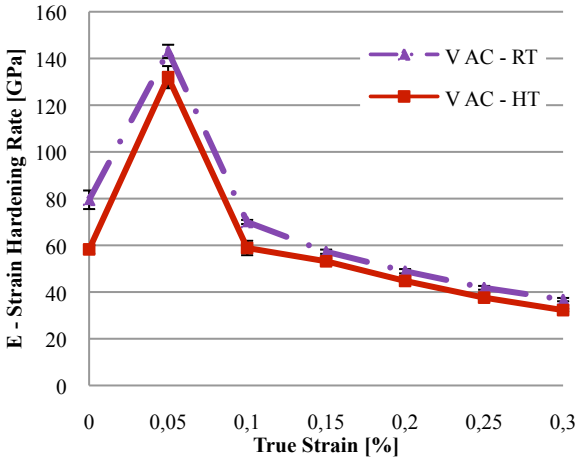

Figure 5.2– *Room temperature vs. High temperature Young's modulus and Strain Hardening Rate (true strain = 0.05%; 0.10%; 0.15%; 0.20%; 0.25% ;0.30%;) of (a) A356 reference, (b) Ni-containing, (c) V-containing sand cast alloys in the as-cast condition. RT and HT in solid and dotted lines respectively.*

In order to justify the increase in yield strength at High Temperature, another hypothesis can be evaluated. A temperature of 235°C and an exposure time of 15 minutes, achieved during the high temperature tensile test, are believed to be sufficient to promote the precipitation of metastable coherent or semi-coherent precipitates, and as a consequence age-hardening occurs. Considering both the absence of solution heat treatment and the short time exposure, the efficiency of the strengthening mechanism is not comparable with traditional heat treatments, consistently with the values of yield strength increase previous discussed (Figures 5.1-2).

5.2.2 The sand cast as-cast Vanadium containing alloys

Casari *et al*. [2] reported that the higher mechanical strength of sand cast V-containing alloys in the as-cast condition (V-AC) was due to solid solution hardening. The V addition into the lattice results in high distortion due to the size difference of the Al and the solute atoms. This reduces the movement of dislocations and cause an increase in yield stress of the material. The stress fields around the solute atoms could interact and eventually ‘’ anchor’’ the dislocations.
At high temperature the internal stress can be recovered by the lattice deformation. As a result the solid solution strengthening is less efficient at 235°C. In fact with respect to the sand cast as-cast material, there is no difference in tensile strength comparing the V-containing with Ni- containing or reference alloys (A 356 AC HT, N AC HT and V AC HT in Figure 4.3).

5.2.3 The T6 condition

The strength of the alloys in the T6 condition Figures 4.4 (sand cast) and 4.6 (permanent mould) show a small decrease at high temperature as compared to the room temperature. As can be seen, UTS drops approximately by 20% for each experimental condition. The heat treatment included solutionising at 540°C for 4 h, quench in water bath at 20°C and aging at 160°C for 6 h. It is believed that 15 minutes holdning at 235°, can promote an over-aging of the precipitates. The over-aging results in a transition from small coherent to large un-coherent precipitates. The dislocation motion is gradually less impeded and eventually the dislocations pass the precipates by looping. As a result the strengths as well as the Hardness decrease. Studies reported that the commercial A356 modified foundry alloy is strongly susceptible to the aging over a temperatures of 200°C [42].

5.3 Fracture behaviour

Figure 4.11 shows the BSE fracture profiles of sand cast reference and Ni- or V- containing alloys in as-cast and T6 condition. Besides the elongation increase approximately by 50% in the high temperature samples, the fracture mode is predominantly brittle, as observed in the room temperature samples [2].The majority of eutectic Si particles still show an elongated acicular morphology even after the solution heat treatment. These elongated eutectic silicon particles frequently generate fracture as they are the main sources of stress concentration [43,44], they will subsequently connect to produce the main crack. Thus, in the absence of modifier elements e.g. Sr or Na, the selected solution heat treatment holding time appears to be insufficient to obtain complete necking and spheroidisation of the Si-particles. SEM fracture investigation of the fracture surface (Figures 4.11-12) is in line with room temperature findings, and confirms the Si-driven quasi cleavage nature of the fracture, as evidenced by the number of cleavage planes and brittle Si-flakes. Few dimples are detected in the fracture surface. No significant differences in the fracture path are observed between the as-cast and the T6 treated alloys.

The alloys studied in this work consist of a soft, low E matrix and hard, high E intermetallics and eutectic Si particles. When these alloys are subject to external loads, an inhomogeneity in stress distribution results from the discrepancy in the elastic properties between the different phases. Similar to a composite material, the stiffer particles generally reinforce the matrix by bearing a larger proportion of the applied load. However if the stress induced at the reinforcing particles or at the matrix-particle interface exceeds a critical value, then fracture of the particles or decohesion occurs [45,46]. Under the high temperature condition, the α-Al matrix is more capable to be deform, the internal stress originated by the non- homogeneity is partially recovered at the expense of the matrix. Hence fracture occurs at lower strength values compared with the room temperature case, but offer higher elongation. After T6 heat treatment, the precipitation of fine coherent Mg_2Si dispersoids in the α-Al matrix exerts a strong effect on the tensile properties of both the sand cast and permanent mould cast samples. Despite this improvement, the α-Al matrix is prone to crack more easily due to the hardening particles, in fact when the fracture of brittle particles begins, the following microcrack linking process is faster and leads to a slightly lower ductility compared to the corresponding as-cast alloys.

6 Conclusion

The influence of Ni and V trace elements on the High temperature tensile properties of as-cast and T6 heat treated A356 unmodified foundry alloys in both sand and permanent mould casting process were studied in the present work. High Temperature tensile tests were performed to evaluate the mechanical properties. Further, microstructural and fractographic investigations were carried out to analyse the microstructures features involved in the fracture process. Finally the High temperature and Room temperature conditions were compared. The following conclusion can be drawn from this study:

- There are no differences between the reference alloy and the Ni- and V- containing alloys. This evidences that neither Ni nor V addition (600 and 1000 ppm respectively) exercises a detrimental effect on the tensile properties.
- Reference and Ni-containing sand and the permanent mould cast samples, in the as-cast condition, evidence that the yield strength increases at High temperature as compared to the Room temperature (by 26% in A356AC and by 138% in N AC). Two hypotheses are proposed. The first one is related to the strain hardening occurring at High temperature where, mutual obstruction of dislocation gliding on intersecting system can be considered a thermally activated process. The second hypothesis is related to the precipitation-hardening mechanism. A temperature of 235°C and an exposure time of 15 minutes, achieved during the high temperature tensile test, are believed to be sufficient to promote the precipitation of metastable coherent or semi-coherent precipitates.
- Room temperature sand cast V-containing samples in the as-cast condition (V-AC) show higher mechanical strength as compared to the reference and Ni-containing samples, due to solid solution hardening exerted by V. At high temperature the internal stress is recovered by the lattice deformation. As a result the solid solution strengthening is less efficient at 235°C.
- The strength of the alloys in the T6 condition, in both sand and permanent mould castings, shows a small decrease at High temperature as compared to the Room temperature. UTS drops approximately by 20% for each experimental condition. It is believed that 15 minutes holding at 235°C, can promote an over-aging of the precipitates.
- SEM fracture investigation of the fracture surface is in line with Room temperature findings, and confirms the Si-driven quasi cleavage nature of the fracture, as evidenced by the number of cleavage planes and brittle Si-flakes. Few dimples are detected in the fracture surface. No

significant differences in the fracture path are observed between the as-cast and the T6 treated alloys.

- Under the high temperature condition, the α-Al matrix is more capable to be deform, the internal stress originated by the non- homogeneity is partially recovered at the expense of the matrix. Hence fracture occurs at lower strength values compared with the room temperature case, but offer higher elongation.

7 Acknowledgement

I would like to express my sincere gratitude to Prof.Lars Arnberg, who hosted my stay at the Norwegian University of Science and Technology (NTNU). His guidance, help, belief in me and suggestions improved my academic skills as much as my personal growth.
Thanks for giving me the chance to join the Solidification and Casting Group and participating in the group seminar in Bergen.
I also very thankful to Prof. Marisa Di Sabatino Lundberg and Prof. Yanjun Li for their precious advises and availability.

I owe my gratitude to my supervisor Prof. Mattia Merlin, who encouraged me to undertake the ‘’Norwegian’’ experience. With is help, trust and patience (dealing with both academicals and bureaucratic matters), he made all this possible and easier.

I want to thank Dr. Daniele Casari for offering me his continuous and reliable support during all my exchange period. His dedication, attention, comprehension taught me ‘’how to walk’’ in the research field. Thanks to be my point of reference.

Special thanks to my fellow roommate Soraia Sofia Pascoa, whit whom I have shared every single moment since the very beginning, for the fact she managed to survive this I will be forever thankful.

I would also like to thank all administrator and laboratory staff at the Department of Material and Technology, for helping me in preparation for my experimental work and for sharing their knowledge and experience about the use of laboratory equipment.

Finally I would like to thanks everyone else who made my period in Trondheim a memorable time.

Bibliography

1. J. Grandfield and J. Taylor, *The impact of rising Ni and V impurity levels in smelter grade aluminum, and potential control strategies*, Material Science Forum, 630.2009, 129-136.

2. D.Casari,T.H.Ludwig, L.Arnberg, M.Merlin and G.L. Garagnani, *"The effect of Ni and V trace elements in as-cast and T6 heat treated conditions*", submitted to Materials Science and Engineering A.

3. W. Kasprzak, D. Emadi, M.Sahoo, M.Aniolek *''Development of Aluminium Alloys for High Temperature Application Diesel Engines''* 10.4028/www.scientific.net/MSF 618-619 pp. 595-600.

4. W. Kasprzak, Z. Deng, J.Powell, M.Niewczas '' *Aging Characteristics, Dimensional Stability and Assessment of High-Temperature Perfomances of Cast Al-Si Alloy for Powertrain applications*'' The Japan Institute of Light Metals pp.669-674.

5. L. Heusler; F.J. Feikus; M.O. Otte, '' *Alloy and Casting Process Optimization for Engine Block Application''* AFS Transactions 01-050, pp.215-223.

6. Z. Asghar, G. Requena, and F. Kubel, "*The role of Ni and Fe aluminides on the elevated temperature strength of an AlSi12 alloy*," Mater. Sci. Eng. A, vol. 527, pp. 5691–5698, 2010.

7. Y. Li, Y. Yang, Y. Wu, L. Wang, and X. Liu, "Quantitative comparison of three Ni-containing phases to the elevated-temperature properties of Al-Si piston alloys," Mater. Sci. Eng. A, vol. 527, pp. 7132–7137, 2010.

8. A. R. Farkoosh, M. Javidani, M. H. D. Larouche, and M. Pekguleryuz, "*Phase formation in as-solidified and heat-treated Al-Si-Cu-Mg-Ni alloys: Thermodynamic assessment and experimental investigation for alloy design*," J. Alloy Compd., vol. 551, pp. 596–606, 2013.

9. A. R. Farkoosh and M. Pekguleryuz, "*The effects of manganese on the T-phase and creep resistance in Al-Si-Cu-Mg-Ni alloys*," Mater. Sci. Eng. A, vol. 582, pp. 248–256, 2013.

10. H. A. Elhadari, H. A. Patel, D. L. Chen, and W. Kasprzak, "*Tensile and fatigue properties of a cast aluminum alloy with Ti, Zr and V additions*," Mater. Sci. Eng. A, vol. 528, pp. 8128–8138, 2011.

11. W. Kasprzak, D. Emadi, M. Sahoo, and M. Aniolek, "*Development of Aluminium Alloys for High Temperature Applications in Diesel Engines*," Mater. Sci. Forum, vol. 618–619, pp. 595–600, 2009.

12. W. Kasprzak, B. S. Amirkhiz, and M. Niewczas, "Structure and Properties of Cast Al-Si based Alloy with Zr-V-Ti Additions and its Evaluation of High Temperature Performance," J. Alloy Compd., 2013.

13. J.F. Hernàndez-Paz, F. Paray, J.E. Gruzleski. AFS Trans. (2004) 155-164.

14. J.L. Murray and A.J. McAlister: Bull. Alloy Phase Diagr., 1984, vol. 5, pp. 74-84.

15. J.G.Kaufmann and E.L. Rooy, Aluminum Alloy Casting: Properties, Process and Applications, ASM International (2004).

16. L.Arnberg L.Bäckerud,G.Chai, *" Solidification Characteristics of Aluminum Alloys"* Vol III,93- 95.

17. M.Merlin, G.L.Garaganani, *"Mechanical and microstructural characterisation of A356 castings realised with full and empty cores "* in Metallurgical Science and Technology , Vol. 27-1, 2009.

18. Couture, A. *"Iron in aluminum casting alloys"*- A literature survey. AFS Int. Cast Met.J., 6(1981), 9-17.

19. Càseres,C.H., Davidson, C.J., Griffiths, J.R., and Q.C.Wang. *"The effect of Mg in the microstructure and mechanical behaviour of Al-Si-Mg castings alloys "*Metall. Mater. Trans. A, 30A (1999), 2611-2618.

20. S. Nafisi, R. Ghomashchi, ''Effect of modification during conventional and semi-solid metal processing of A356 Al-Si alloy'', Materials Science and Engineering A, 415, 1-2, pp. 273-28.

21. L.F. Mondolfo, *Aluminum Alloys : structure and properties*. 1976, London: Butterwhorths.

22. K.T.Kashyap, S.Murali, K.S.Raman and K.S.S.Murthy, ibid.9 (1993), pp. 189-190.

23. A. M. Samuel, J. Gauthier, F. H. Samuel, *''Microstructural aspects of the dissolution and melting of Al2Cu phase in Al-Si alloys during solution heat treatment''* Metallurgical and Materials Transactions A. July 1996, Volume 27, Issue 7, pp 1785-1798.

24. A.M.A. Mohamed, and F.H. Samuel, ''A Review on the Heat Treatment of Al-Si-Cu/Mg Casting Alloys'' Intech, 2012.

25. S. Shivkumar, C. Keller, D. Apelian *'' Aging behavior in cast alumimium alloys''* ; AFS Trans, 179 (1990), p.p. 905-911.

26. Apelian et al.1990 American Foundry Society, Schaumburg, Illinois, USA.

27. G.Jha, F.Cannova, and B.Sadler, *" Is this Really a Problem for Metal Quality?"* in LIGHT METALS 2012, C.E.Suarez,Ed. TMS,2012, pp. 1303-1306.

28. J.Grandfield, L.Sweet, C.Davidson, J.Mitchell, A.Beer, S.Zhu, X.Chen, and M. Easton: *"An initial assessment of the effects of increased Ni and V in A356 and AA6036"* Light Metal 2013, 2013, 39-45.

29. S.Zhu, J.-Y.Yao, L. Swee, M.Easton, J.Taylor, P.Robiso, and N.Parson : *"Influences of Nickel and Vanadium Impurities on Microstructure of Aluminum alloys",* JOM, 2013, vol.65, pp. 584-592.

30. Garci, J.A. Hinojosa, C.R. Gonzalez, C.M. Gonzalez and Y.Houbaert: J.Mater.Process.Tech.,2003, vol. 143-144, pp. 306-310.

31. 12 T.H. Ludwig, P.L.Schaffer, L.Arnberg : *"Influences of Some trace elements on Solidification Path and Microstructure of Al-Si Foundry Alloys"* Metall. Mater. Trans. A, vol. 44A(2013), pp.3783-3796.

32. 2.13 F.Stadler, H.Antrekowitsch, W. Fragner, H. Kaufmann, and P.J. Uggowitzer: Mater. Sci. Forum, 2011, vol.690,pp. 27-277.

33. I.J.Polmear.Light Alloys: From Traditional Alloys to Nanocrystals Butterworth-Heinemann, 2005, pp 30-31.

34. U. Mannweiler, W. Schmidt-Hatting, D. Rodriguez, and A. Maitland.''*High Vanadium Venezuelan Petroleum Coke, A Rawmaterial for the Aluminum Industry?*'' Light Metals,1989, pp 449-454.

35. L.F. Mondolfo, *Aluminum Alloys : structure and properties*. 1976, London: Butterworth.

36. H.A. Elhadari, H.A. Patel, D.L. Chen, W. Kasprzak: Mat.Sci. Eng.A,2011, vol 528, pp.867-872.

37. T.H. Ludwig, P. Schaffer, L. Arnberg. *The Influence of Vanadium on the Microstructure of A356 Foundry Alloy*. · TMS Light Metals 01/2013.

38. Hot Tension and Compression Testing. ASM Handbook, Volume 08 - Mechanical Testing and Evaluation.

39. X. Q. Shi, W. Zhou*, H. L. J. Pang*, and Z. P. Wang . Effect of Temperature and Strain Rate on Mechanical Properties of 63Sn/37Pb Solder Alloy. ASME Journal of Electronic Packaging, ASME, USA, Vol. 121, No. 3, 1999, lpp. 179-185.

40. D.McLean,`` Mechanical Properties of Metals``, John Wiley & Sons, Inc.,1962,pp.153-161.

41. 5.2 M.A. Meyers and K.K. Chawla,``Mechanical Metallurgy``, Prentice-Hall, Inc., Englewood Cliffs, N.J., 1984.

42. L. Ceschini, A. Jarfors, Al. Morri, An. Morri, F. rotundo, S. Seifeddine, *High temperature tensile behaviour of the A354 aluminum alloy,* L. Ceschini, A. Jarfors, Al. Morri, An. Morri, F. rotundo, S. Seifeddine, ICAA 2014.

43. Wang Q. G., Casaeres C. H., Grifhits J R.'' *Damage by eutectic particle cracking in aluminum casting alloys A356/357 ''.* Metallurgical and Materials Transactions A, 2003, 34(12): 2901−2912.

44. Fadavi I., Boostani A., Tamanthas S.,'' *Fracture behavior of thixoformed A356 alloy produced by SIMA processAlloys and Compounds''* 2009, 481(1−2): 220−227.

45. I.Sinclair and P.J.Gregson,''*Structural performances of discontinuous metal matrix composit'',* Mater. Sci. Techonol. Vol.13, pp 709-726,1997.

46. M.Huang and Z.Li, '' *Influences of particle size and interface energy on the stress concentration induced by the oblate spherozied particles and the void nucleation mechanism''*, Int. Solid. Struct., vol 43, pp.634-641,2009.